

Supporting information for

The role of β -hairpin conformation in ester hydrolysis peptide catalysts based on a TripZip scaffold

Xinyu Liu,^a Riley Waters,^b Hannah E. Gilbert,^b Gage Barroso,^b Kelsey M. Boyle,^b and Leah S. Witus*^b

^a Department of Chemistry, University of Wisconsin-Madison, Madison, Wisconsin 53706, USA.

^b Department of Chemistry, Macalester College, Saint Paul, Minnesota 55105, USA.

*Correspondence should be addressed to L.S.W. (lwitus@macalester.edu)

Table of Contents

DATA ON 10MER PEPTIDE SERIES WITH TRUNCATED N- AND C-TERMINI.....	2
NMR EXPERIMENTS	5
<i>a) 1D ¹H, 2D TOCSY, and 2D NOESY NMR Data</i>	<i>5</i>
<i>b) NMR proton assignments and NOE/ROE analysis.....</i>	<i>15</i>
CIRCULAR DICHROISM	20
PEPTIDE CHARACTERIZATION	21
COMPUTATIONAL MODELS	33
SUPPLEMENTAL REFERENCES	34

Data on 10mer peptide series with truncated N- and C-termini

Sequences based on the TrpZip sequence with a truncation of the N- and C-terminal residues were also studied. In these 10mer sequences (listed in Table S1) the cross-strand positioning of the catalytic residues was in positions 2 and 9. Chemical shift deviation (CSD) analysis of sequences **Trunc-TrpZip**, **Trunc-2H9H-pG**, and **Trunc-2H9H-PG**, showed some positive deviations indicative of β -hairpin character in the D-Pro-Gly-containing **Trunc-2H9H-pG**, but not in the L-Pro-Gly-containing **Trunc-2H9H-PG** or **Trunc-TrpZip** (Figure S1). The catalytic efficiency of these sequences showed similar trends to the full-length sequences discussed in the main text (Figures S2-4).

Table S1. 10mer peptide sequences studied. The N-termini were free amines and the C-termini were amidated. Lowercase one letter code indicates use of D amino acid.

<i>peptide</i>	<i>sequence</i>
Trunc-TrpZip	NH ₂ -WTWEGNKWTW-NH ₂
Trunc-2H9H-pG	NH ₂ -WHWEpGKWHW-NH ₂
Trunc-2H9H-PG	NH ₂ -WHWEPGKWHW-NH ₂
Trunc-2H9K-pG	NH ₂ -WHWEpGKWKW-NH ₂
Trunc-2H9K-PG	NH ₂ -WHWEPGKWKW-NH ₂

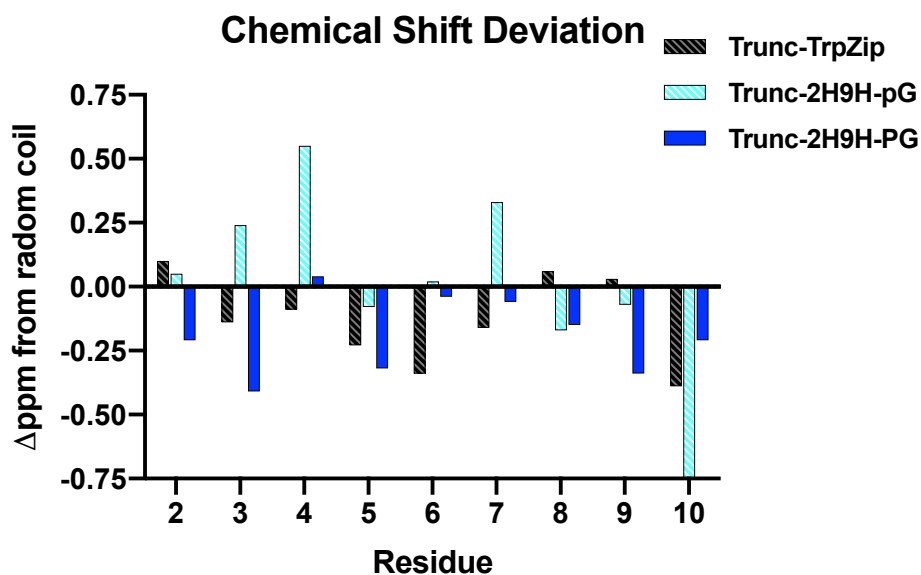


Figure S1. CSD analysis of the 10mer peptide sequences.

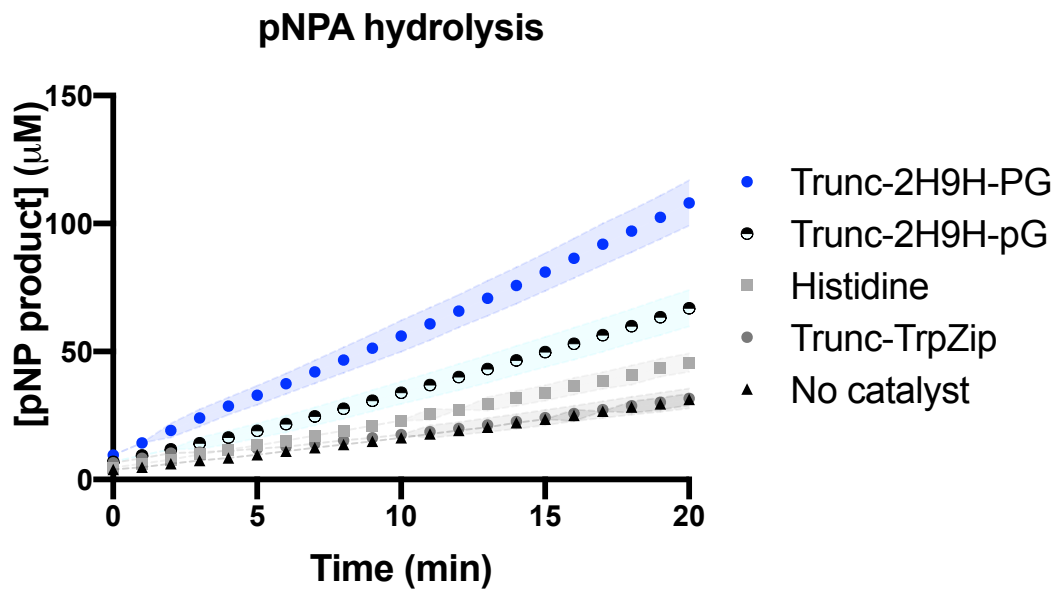


Figure S2. pNPA hydrolysis plot wherein the shaded areas represent the area between error bars from 9 replicates in three separate experiments.

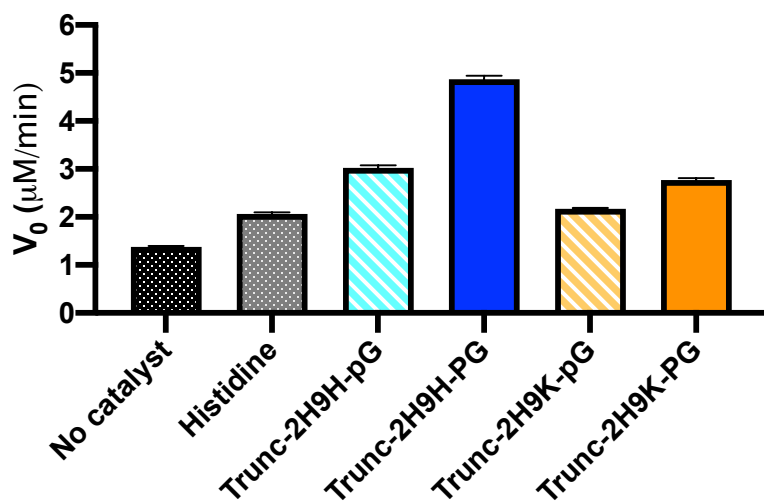


Figure S3. A comparison of initial velocity of each sequence of the 10mer series of peptides.

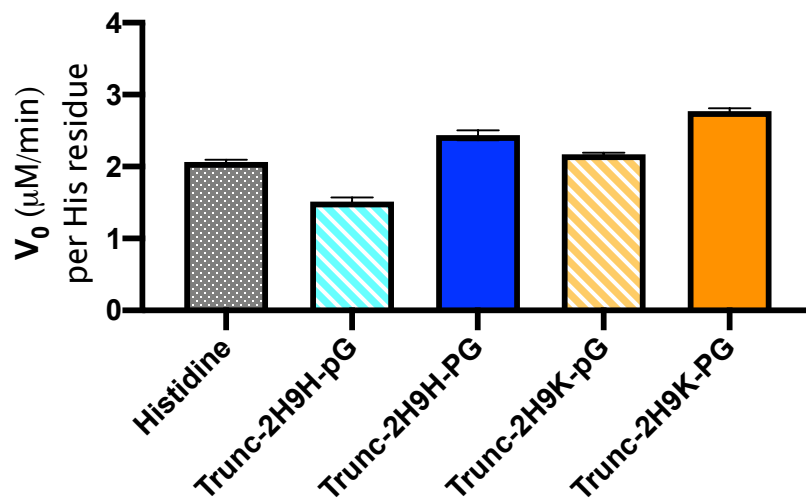


Figure S4. A comparison of the initial velocity for each catalyst on a per histidine equivalent basis.

NMR experiments

Peptide samples were analyzed with a Bruker Avance 600MHz spectrometer equipped with a 5mm,z-axis gradient, triple resonance, cryogenic probe. Peptides were dissolved in 600 μ L of 9:1 H₂O:D₂O at a concentration of 1 mM with trace amounts of 2,2-dimethyl-2-silapentane-5-sulfonate (DSS) as internal reference. All spectra were obtained at 24°C. The following standard Avance pulse programs were employed: 1D with solvent suppression using excitation sculpting (zgesgp), 2D TOCSY with excitation sculpting (mlevesgp), 2D NOESY with excitation sculpting (noesyegpph), and 2D ROESY with excitation sculpting (roesyegpph). TOCSY experiments used a mixing time of 100 ms. NOESY experiments used a mixing time of 250 ms. ROESY experiments used a mixing time of 300 ms. Data were processed using TopSpin 3.6.1. Data were analyzed using MestRe Nova 12.0.1 and NMRFAM Sparky^{S1}, with employment of sequential assignment procedures to assign chemical shifts of protons.

a) 1D ¹H, 2D TOCSY, and 2D NOESY NMR Data

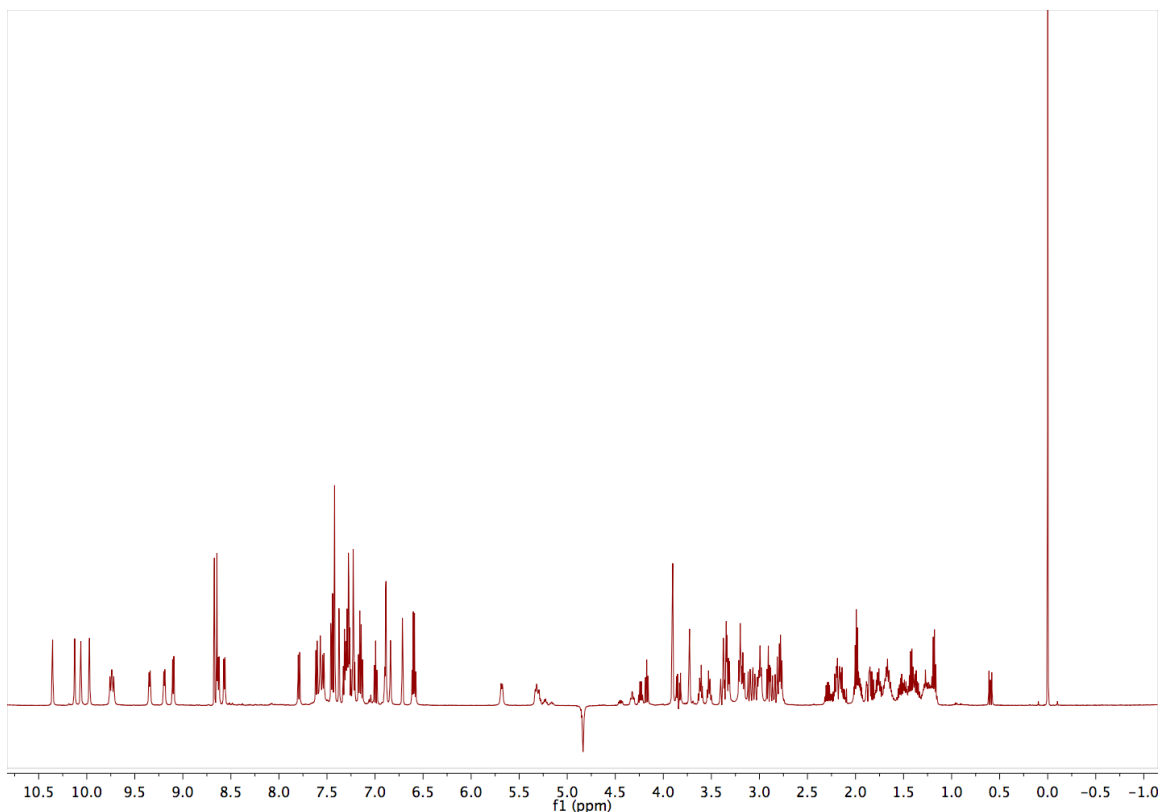


Figure S5: Solvent-suppressed ¹H-NMR of 3H10H-pG in 9:1 H₂O:D₂O at 1 mM.

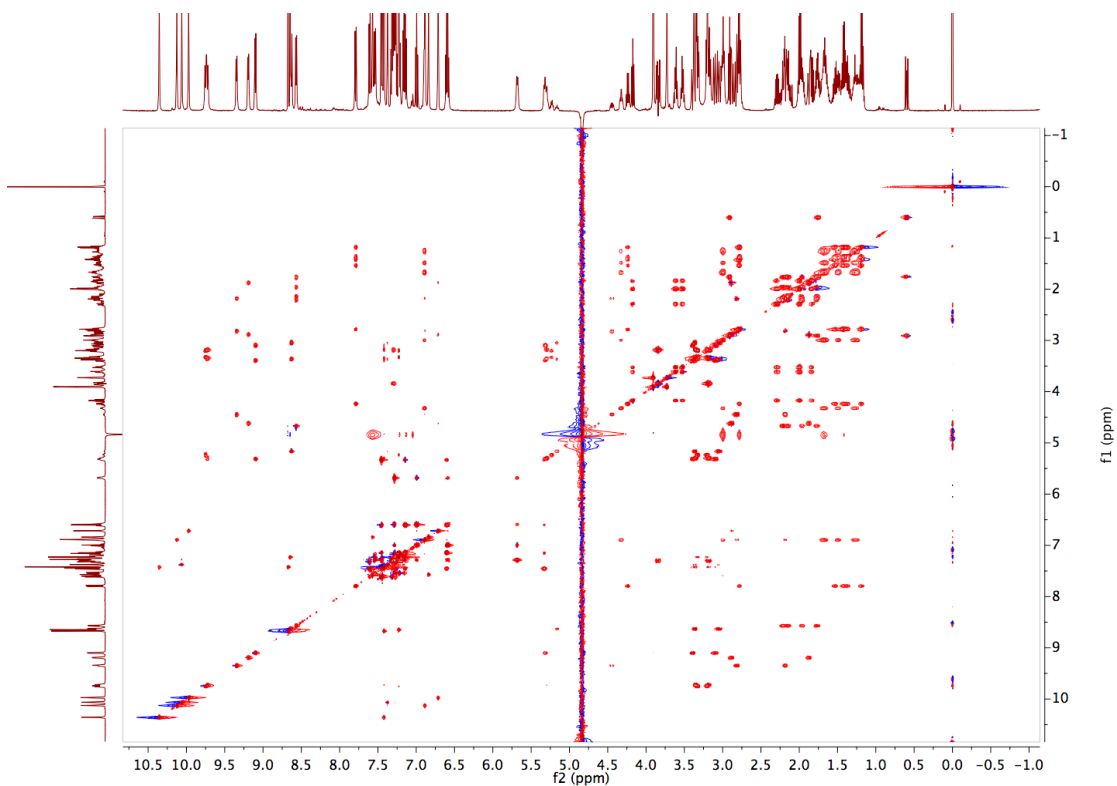


Figure S6: Solvent-suppressed 2D TOCSY NMR of **3H10H-pG** in 9:1 H₂O:D₂O at 1 mM.

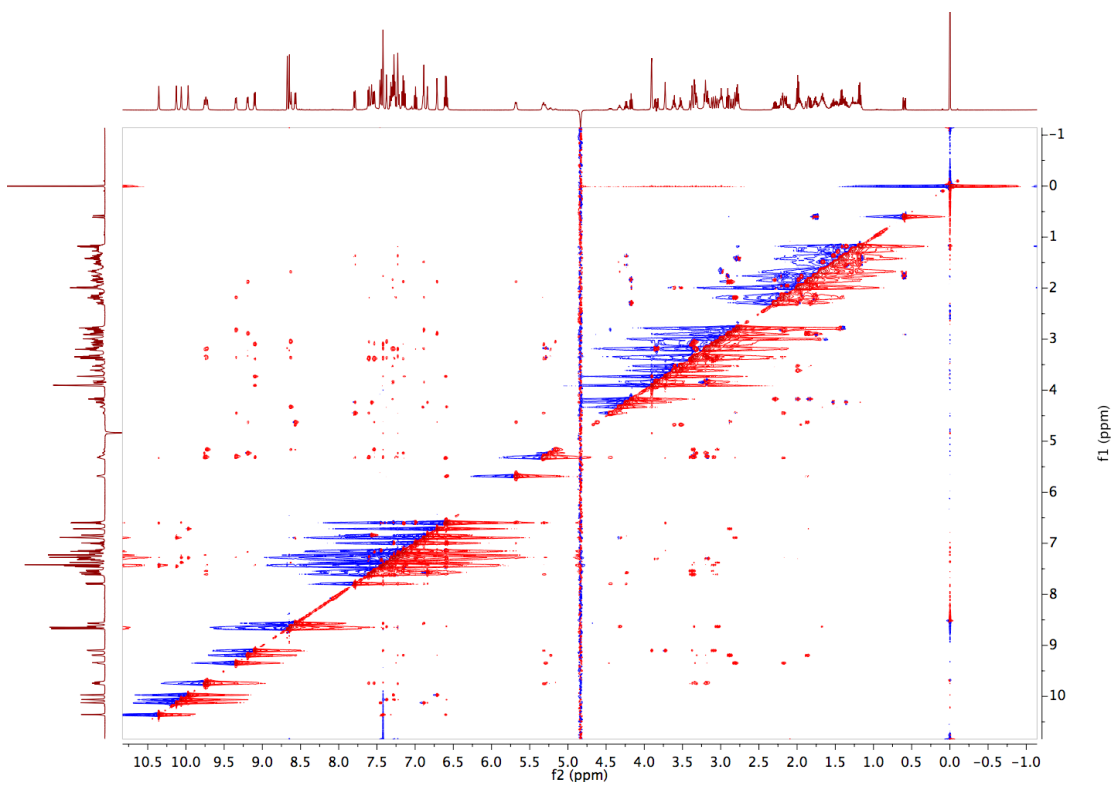


Figure S7: Solvent-suppressed 2D NOESY NMR of **3H10H-pG** in 9:1 H₂O:D₂O at 1 mM.

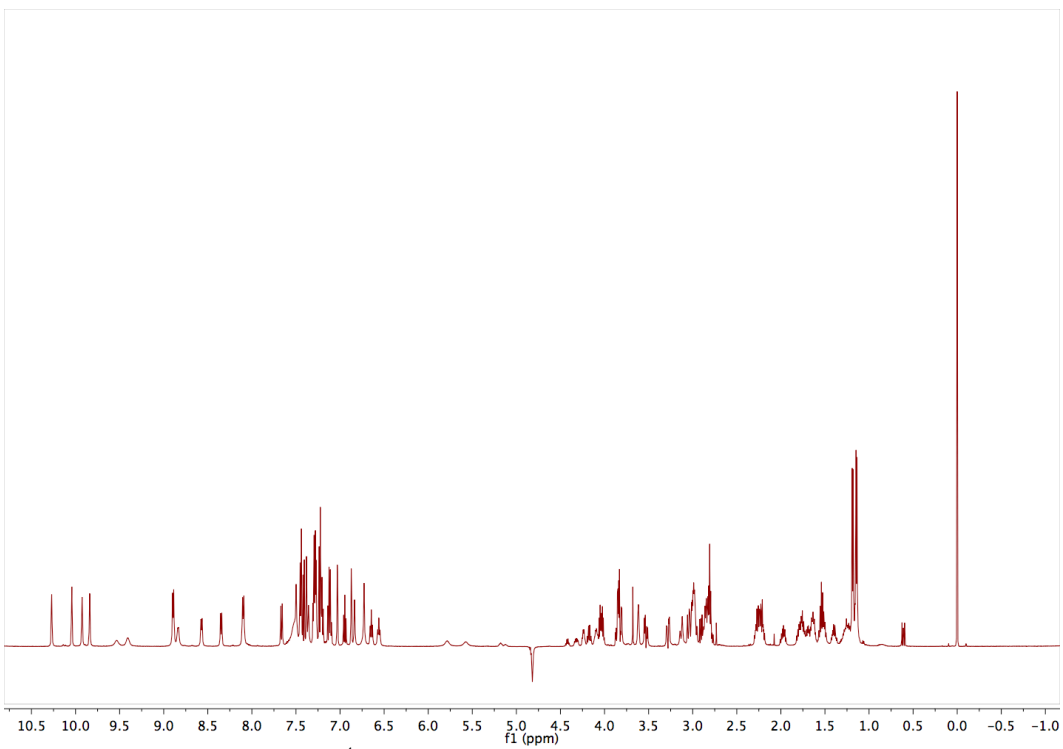


Figure S8: Solvent-suppressed ¹H-NMR of TrpZip in 9:1 H₂O:D₂O at 1 mM.

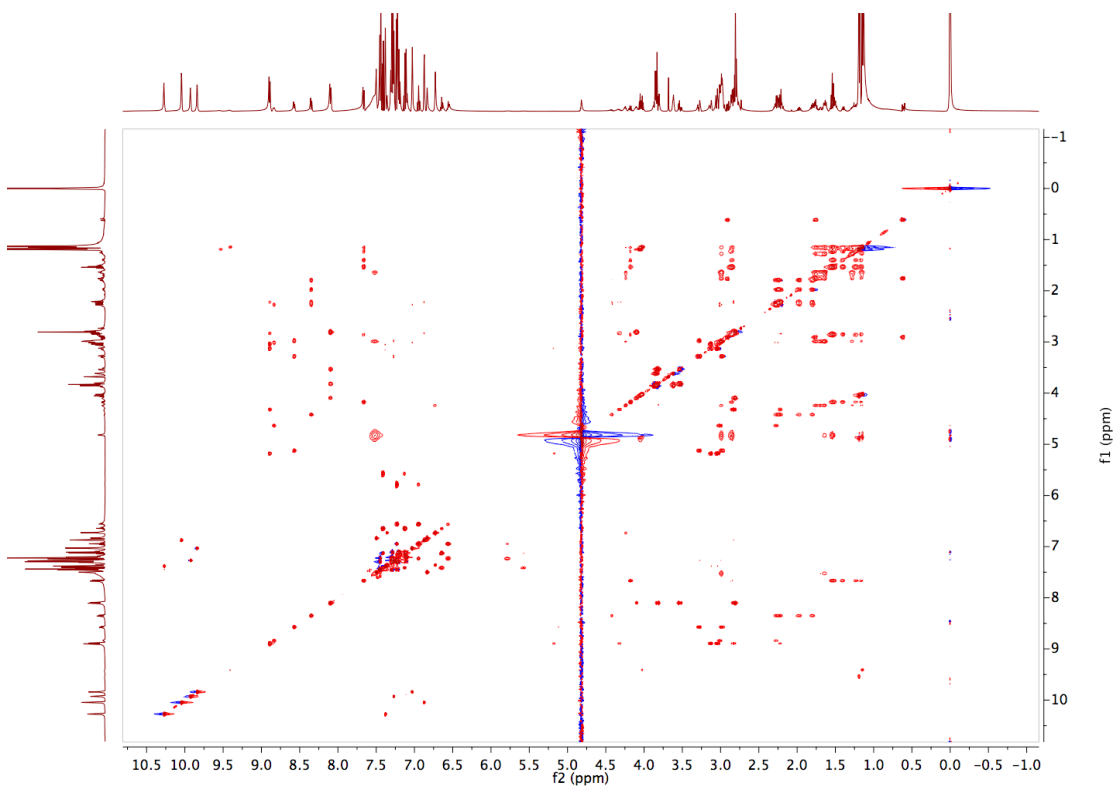


Figure S9: Solvent-suppressed 2D TOCSY NMR of TrpZip in 9:1 H₂O:D₂O at 1 mM.

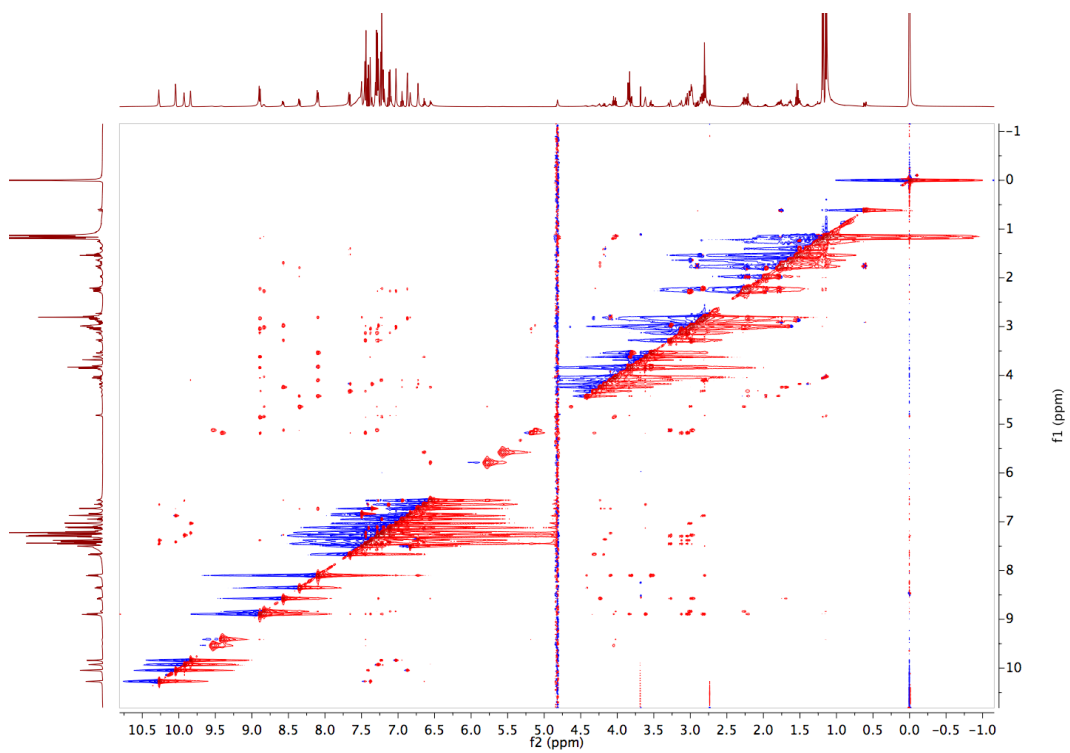


Figure S10: Solvent-suppressed 2D NOESY NMR of **TrpZip** in 9:1 H₂O:D₂O at 1 mM.

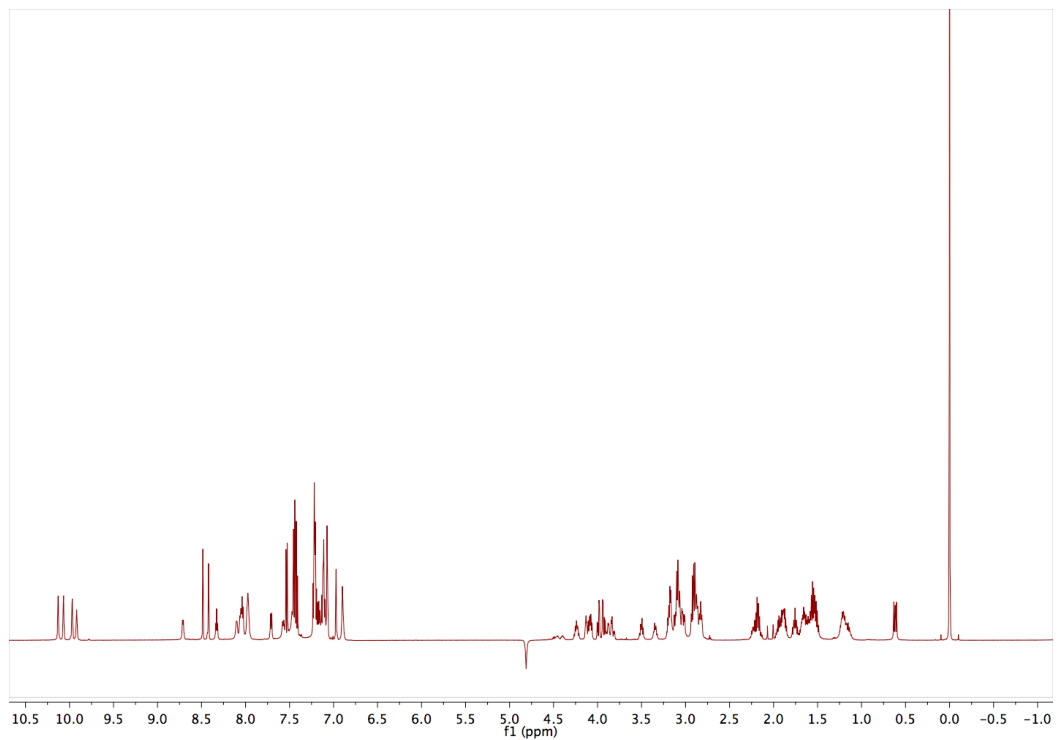


Figure S11: Solvent-suppressed ¹H-NMR of **3H10H-PG** in 9:1 H₂O:D₂O at 1 mM.

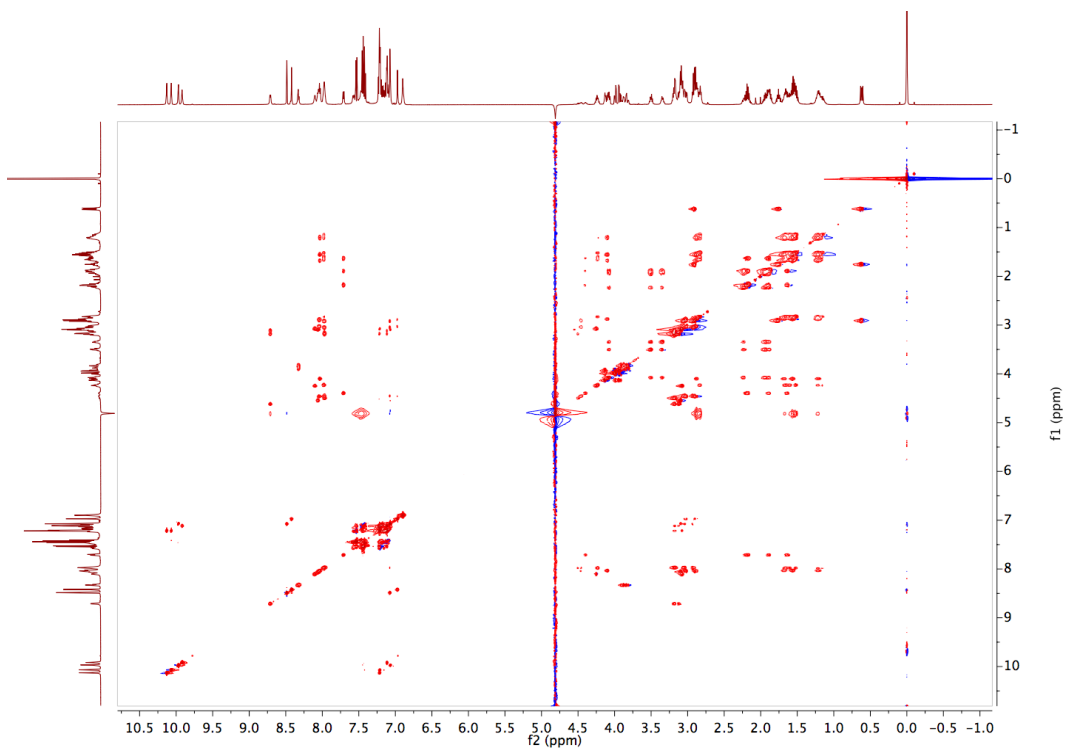


Figure S12: Solvent-suppressed 2D TOCSY NMR of **3H10H-PG** in 9:1 H₂O:D₂O at 1 mM.

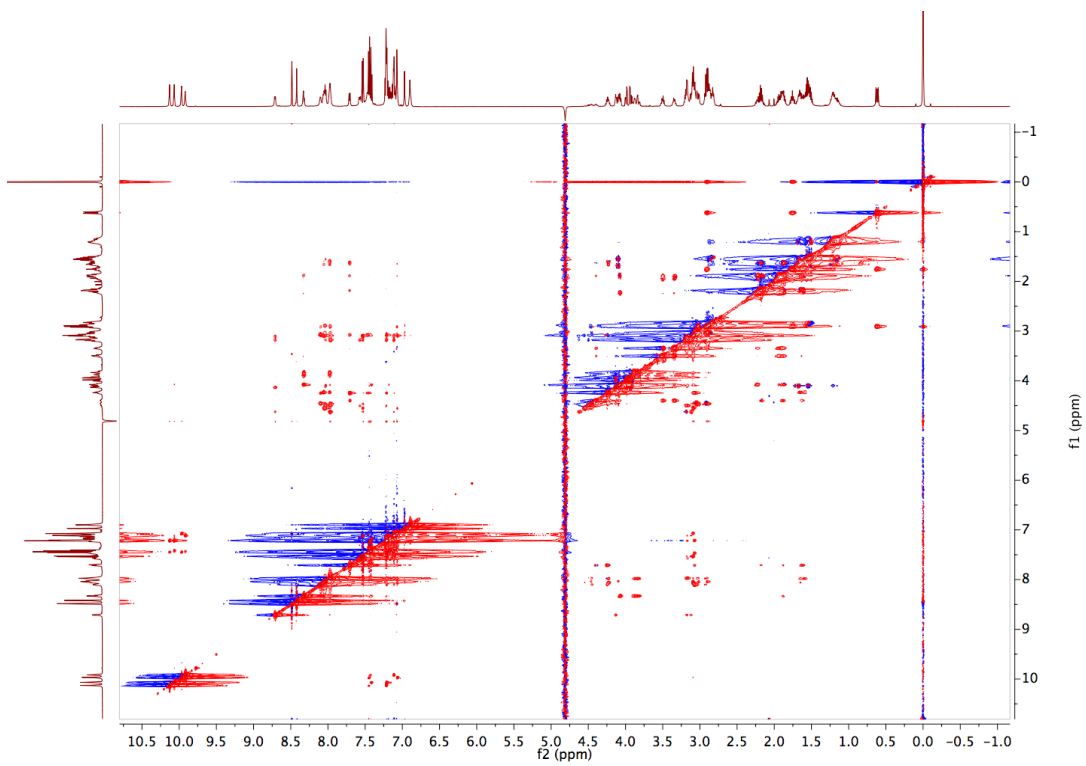


Figure S13: Solvent-suppressed 2D NOESY NMR of **3H10H-PG** in 9:1 H₂O:D₂O at 1 mM.

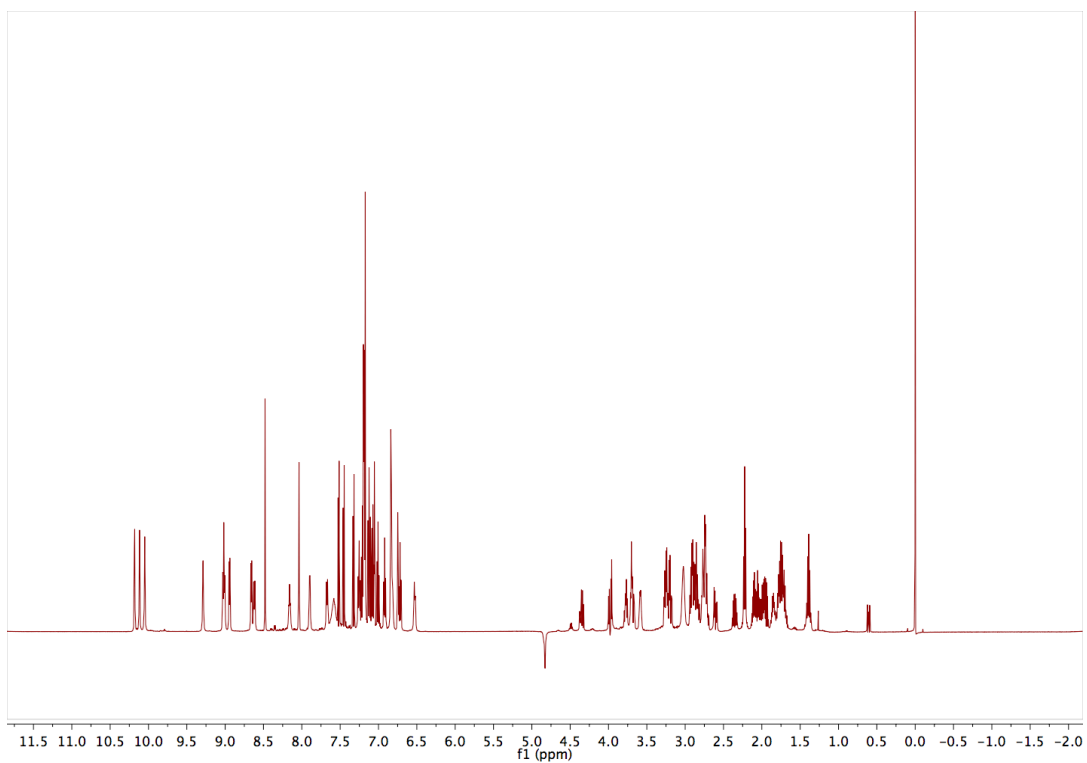


Figure S14: Solvent-suppressed $^1\text{H-NMR}$ of **Trunc-2H9H-pG** in 9:1 $\text{H}_2\text{O}:\text{D}_2\text{O}$ at 1 mM.

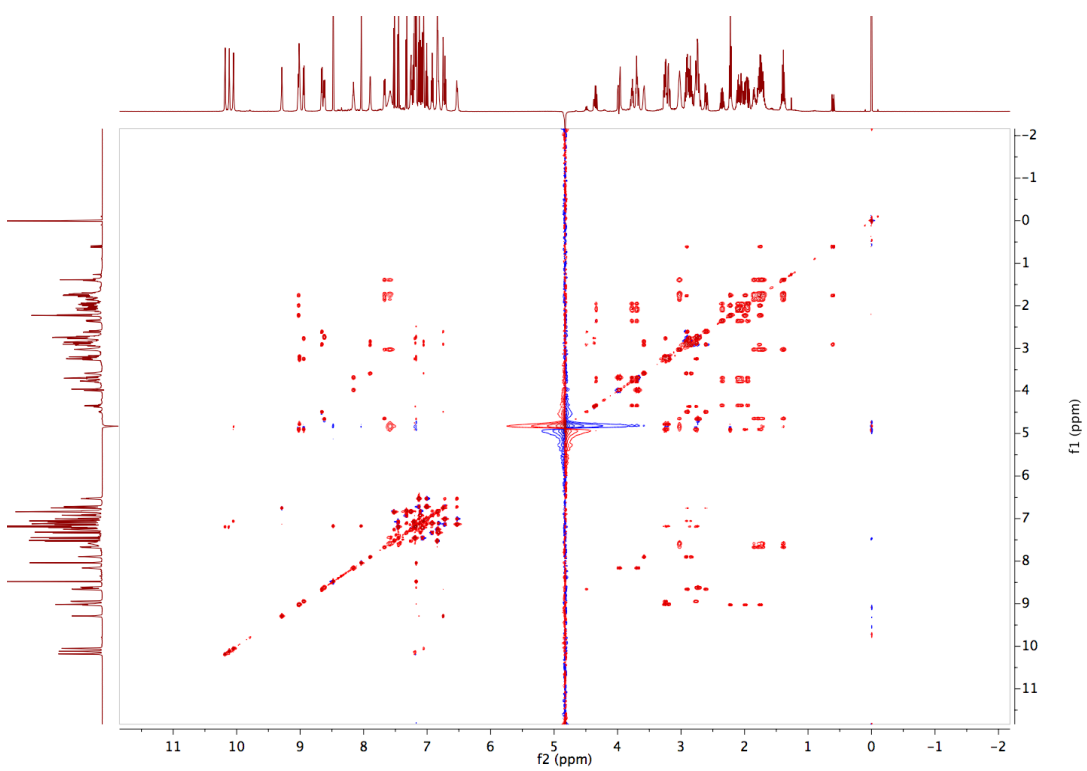


Figure S15: Solvent-suppressed 2D TOCSY NMR of **Trunc-2H9H-pG** in 9:1 $\text{H}_2\text{O}:\text{D}_2\text{O}$ at 1 mM.

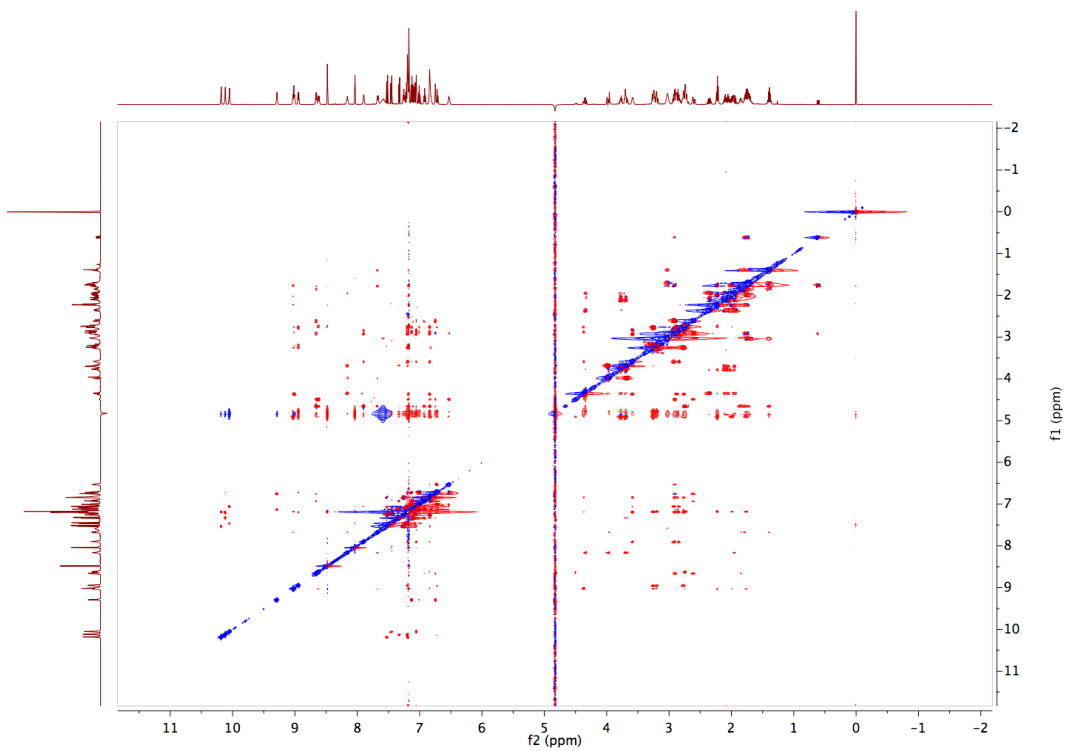


Figure S16: Solvent-suppressed 2D ROESY NMR of **Trunc-2H9H-pG** in 9:1 H₂O:D₂O at 1 mM.

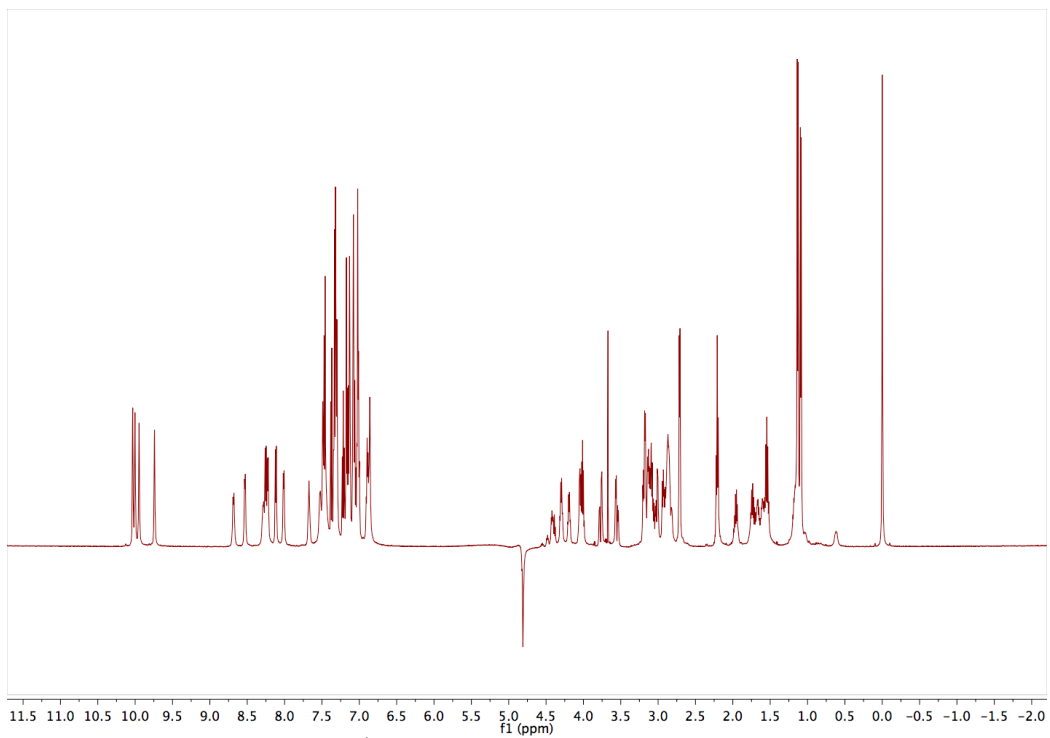


Figure S17: Solvent-suppressed ¹H-NMR of **Trunc-TrpZip** in 9:1 H₂O:D₂O at 1 mM.

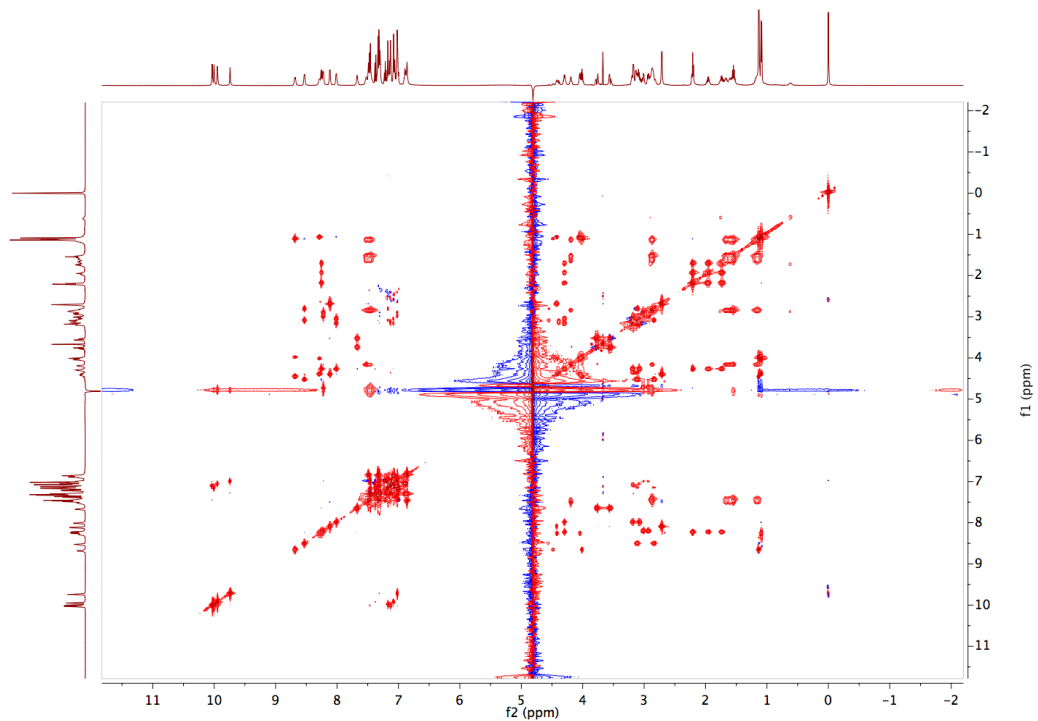


Figure S18: Solvent-suppressed 2D TOCSY NMR of **Trunc-TrpZip** in 9:1 H₂O:D₂O at 1 mM.

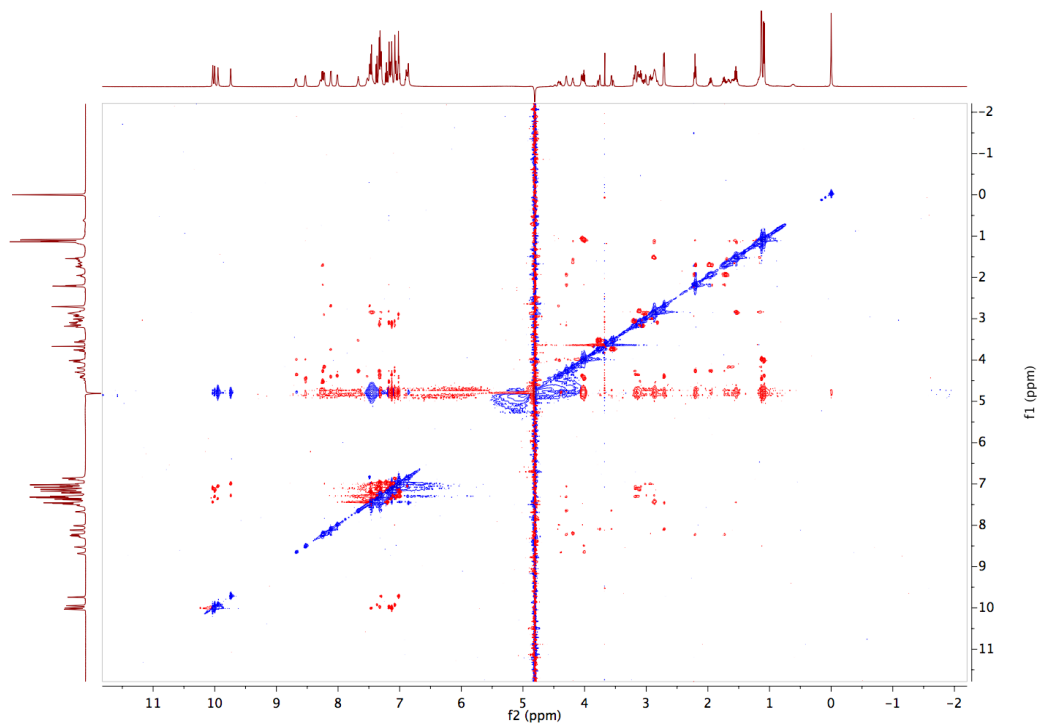


Figure S19: Solvent-suppressed 2D ROESY NMR of **Trunc-TrpZip** in 9:1 H₂O:D₂O at 1 mM.

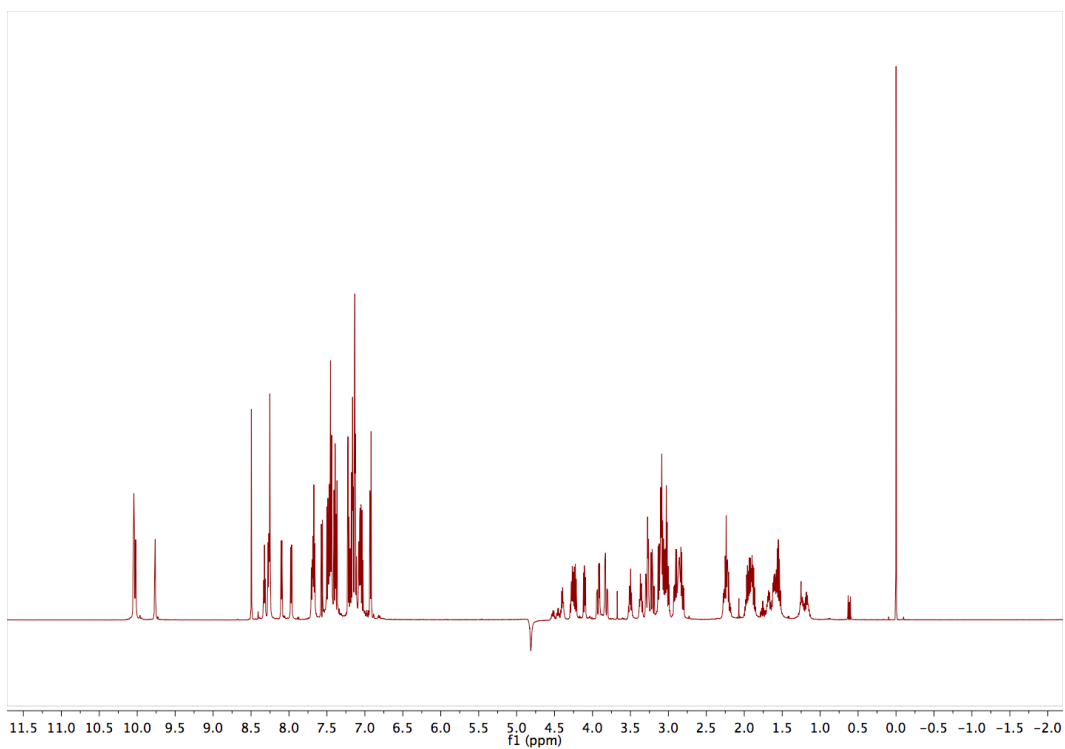


Figure S20: Solvent-suppressed $^1\text{H-NMR}$ of **Trunc-2H9H-PG** in 9:1 $\text{H}_2\text{O}:\text{D}_2\text{O}$ at 1 mM.

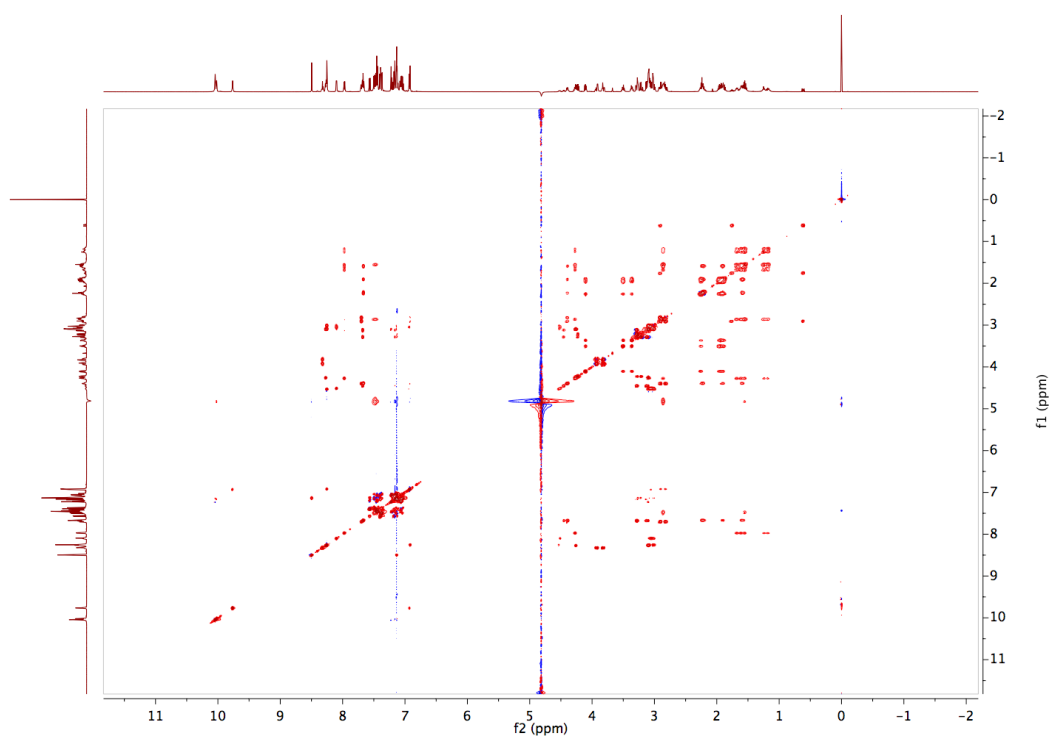


Figure S21: Solvent-suppressed 2D TOCSY NMR of **Trunc-2H9H-PG** in 9:1 $\text{H}_2\text{O}:\text{D}_2\text{O}$ at 1 mM.

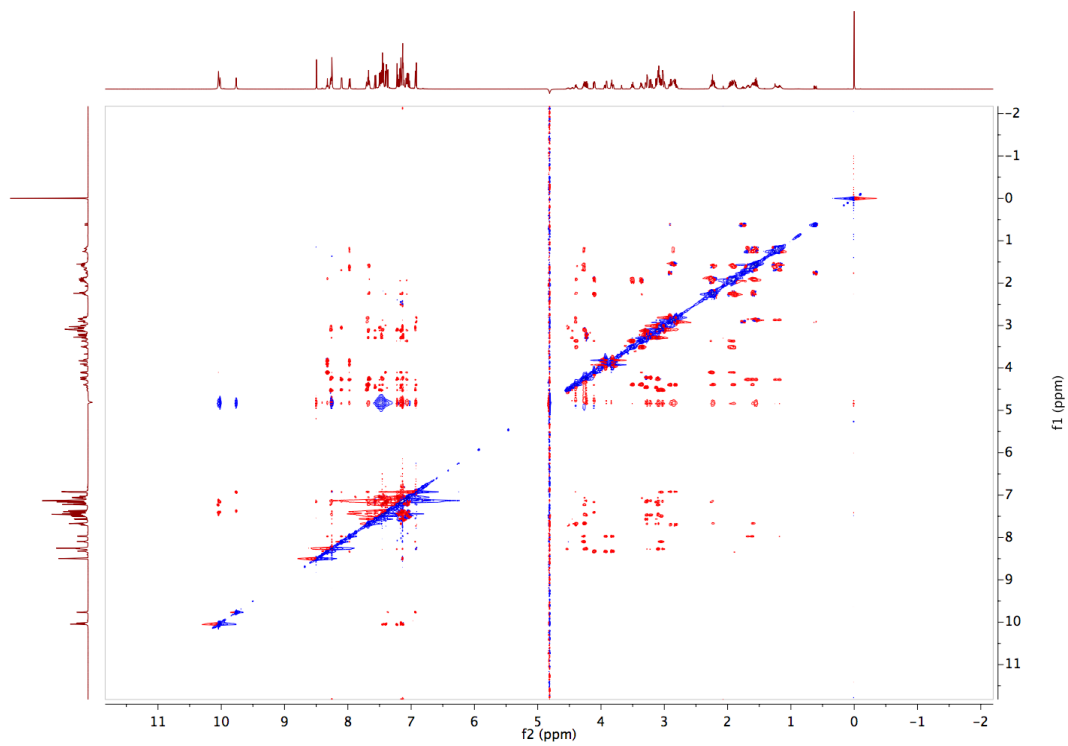


Figure S22: Solvent-suppressed 2D NOESY NMR of **Trunc-2H9H-PG** in 9:1 H₂O:D₂O at 1 mM.

b) NMR proton assignments and NOE/ROE analysis

Table S2. Proton resonances (ppm) for **3H10H-pG**.

	HN	H α	H β	H γ	H δ	H ϵ	Other
Ser1			3.91, 3.73				
Trp2	9.10	5.31	3.39, 3.10		7.42	10.36	H ϵ 3: 7.27; H ζ 3: 7.45; H η 2: 7.14; H ζ 2: 6.60
His3	9.75	5.23	3.33, 3.20		7.23	8.65	
Trp4	9.19	4.62	2.89, 1.87		6.72	9.98	H ζ 2: 7.29
Glu5	8.57	4.67	1.96, 1.76	2.21, 2.15			
DPro6	NA	4.174	2.30, 1.99	1.83	3.61, 3.53		
Gly7	7.29	3.84, 3.18					
Lys8	6.89	4.32	1.68	1.26	1.49	3.00	
Trp9	8.63	5.17	3.36, 3.05		7.38	10.07	H ζ 2: 6.59
His10	9.72	5.31	3.37, 3.18		7.42	8.67	
Trp11	9.34	4.44	2.82, 2.18		6.89	10.14	H ζ 2: 7.45
Lys12	7.79	4.24	1.54	1.19	1.42, 1.37	2.78	

Table S3. NOEs observed for **3H10H-pG** (signals for sequence assignment are excluded).

NOE Assignments	CS1(ppm)	CS2(ppm)
Trp11HA-His3HD2	4.44	7.23
Trp11HA-His3HN	4.44	9.75
Lys12HB-His3HD2	1.54	7.23
Lys12HD3-His3HD2	1.37	7.23
Lys12HG-His3HD2	1.19	7.23
His3HB3-Lys12HG	3.20	1.19
His3HB2-Lys12HG	3.33	1.19
Trp4HA-His10HN	4.62	9.72
Glu5HB3-His10HD2	1.76	7.42

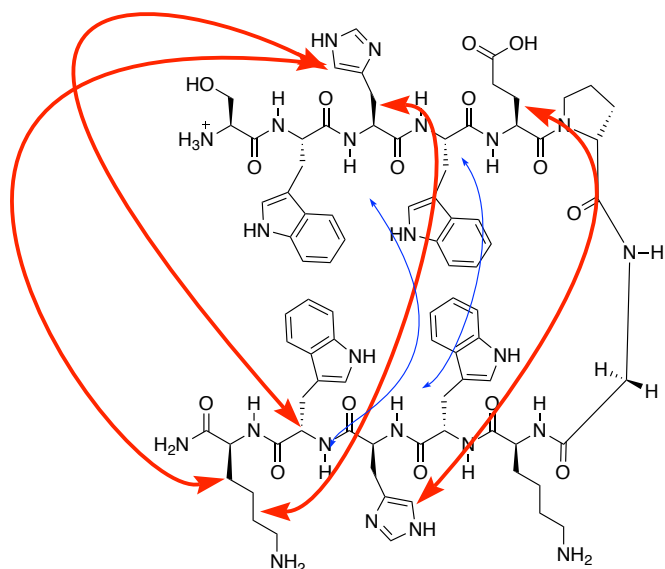


Figure S23: Selected NOEs for **3H10H-pG**. Red arrows indicate a long-range NOEs involving side chains. Blue arrows indicate long-range backbone NOEs.

Table S4. Proton resonances (ppm) for **TrpZip**.

	HN	H α	H β	H γ	H δ	H ϵ	Other
Ser1			3.84, 3.62				
Trp2	8.89	5.18	3.12, 3.04		7.38	10.27	H ϵ 3: 7.45; H η 3: 6.73; H ζ 2: 6.65
Thr3	9.41	4.84	4.02	1.14			
Trp4	8.84	4.64	3.01, 2.27		7.04	9.84	H ζ 2: 7.23
Glu5	8.35	4.42	1.98, 1.79	2.26, 2.22			
Gly6	8.10	3.84, 3.53					
Asn7	8.10	4.10	2.81				
Lys8	6.73	4.24	1.76, 1.70	1.28, 1.55	1.64	2.99	NH2 ζ : 7.52
Trp9	8.57	5.13	3.28, 2.98		7.27	9.93	H ζ 2: 6.56
Thr10	9.53	4.86	4.05	1.19			
Trp11	8.89	4.32	2.83, 2.27		6.87	10.04	H ζ 2: 7.43
Lys12	7.66	4.17	1.53	1.23, 1.16	1.40	2.86	NH2 ζ : 7.52

Table S5. Proton resonances (ppm) for **3H10H-PG**.

	HN	Hα	Hβ	Hγ	Hδ	Hϵ	Other
Ser1			4.13				
Trp2	8.71	4.62	3.18, 3.12		7.11	9.92	H ζ 2: 7.43
His3	7.97	4.45	3.04, 2.92		7.08	8.49	
Trp4	8.10	4.25	3.08		7.07	9.97	H ζ 2: 7.45
Glu5	7.71	4.39	1.89, 1.63	2.18			
Pro6		4.08	2.23	1.90	3.50, 3.35		
Gly7	8.33	3.88, 3.84					
Lys8	7.98	4.23	1.65, 1.60	1.21, 1.15	1.52	2.83	NH2 ζ : 7.46
Trp9	8.06	4.55	3.09		7.21	10.07	H ϵ 3: 7.53; H ζ 2: 7.42
His10	8.04	4.46	3.02, 2.89		6.97	8.42	
Trp11	7.97	4.50	3.17, 3.07		7.22	10.13	H ζ 2: 7.45
Lys12	8.03	4.10	1.68	1.21	1.56	2.87	NH2 ζ : 7.46

Table S6. Proton resonances (ppm) for **Trunc-2H9H-pG**.

	HN	Hα	Hβ	Hγ	Hδ	Hϵ	Other
Trp1		4.37	2.87, 2.75		7.21	10.12	H ζ 2: 7.33
His2	9.01	4.78	3.25, 3.19		7.17	8.04	
Trp3	8.94	4.90	3.25, 2.76		7.19	10.18	H ζ 2: 7.52
Glu4	9.02	4.90	1.99, 1.75	2.23			
D-Pro5		4.34	2.35, 2.10	2.05, 1.95	3.77, 3.70		
Gly6	8.16	3.98, 3.68					
Lys7	7.67	4.65	1.85, 1.78	1.39	1.73	3.02	NH2 ζ : 7.58
Trp8	8.66	4.49	2.91, 2.60		6.75	9.3	H ζ 2: 7.13
His9	8.62	4.66	2.73		7.18	8.48	
Trp10	7.89	3.59	2.92, 2.84		7.06	10.05	H ζ 2: 7.46

Table S7. ROEs observed for **Trunc-2H9H-pG** (signals for sequence assignment are excluded).

ROE Assignments	CS1(ppm)	CS2(ppm)
Trp1HA-Trp10HA	4.37	3.59
His9HN-His2HN	8.62	9.01
His9HE-Glu4HG	8.48	2.23
His9HE-Glu4HB	8.48	1.75

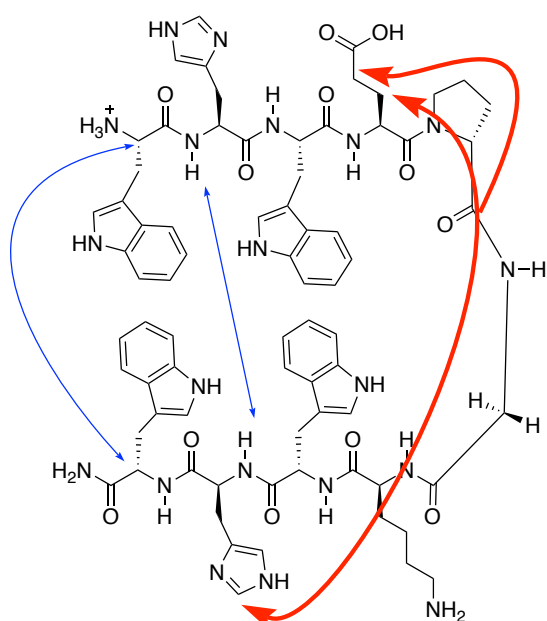


Figure S24: Selected ROEs for **Trunc-2H9H-pG**. Red arrows indicate long-range ROEs involving side chains. Blue arrows indicate long-range backbone ROEs.

Table S8. Proton resonances (ppm) for **Trunc-TripZip**.

	HN	Hα	Hβ	Hγ	Hδ	Hϵ	Other
Trp1		4.36	3.13		7.13	10.04	H ζ : 7.43
Thr2	8.68	4.45	3.98	1.1			
Trp3	8.53	4.52	3.08, 2.81		7.18	10.01	H ζ : 7.29
Glu4	8.26	4.26	1.93, 1.70	2.18			
Gly5	7.67	3.73, 3.52					
Asn6	8.12	4.4	2.68				
Lys7	7.53	4.16	1.63, 1.57	1.13	1.52	2.84	NH 2ζ : 7.46
Trp8	8.22	4.72	2.98, 2.90		7.02	9.74	H ζ : 7.28
Thr9	8.28	4.38	4.01	1.06			
Trp10	8.02	4.27	3.15,3.05		7.08	9.95	H ζ :7.34

Table S9. Proton resonances (ppm) for **Trunc-2H9H-PG**.

	HN	Hα	Hβ	Hγ	Hδ	Hϵ	Other
Trp1		4.23	3.27, 3.21		7.14	10.04	H ζ : 7.45
His2	8.25	4.52	3.09, 3.01		7.13	8.49	
Trp3	8.27	4.25	3.09		7.23	10.05	H ζ : 7.40
Glu4	7.67	4.39	1.90, 1.58	2.22			
Pro5		4.10	2.25	1.95, 1.89	3.50, 3.36		
Gly6	8.32	3.92, 3.82					
Lys7	7.97	4.27	1.68	1.24, 1.17	1.60, 1.55	2.85	NH 2ζ : 7.48
Trp8	8.10	4.51	3.04		6.94	9.77	H ζ : 7.37
His9	7.70	4.39	2.90, 2.81		6.92	8.25	
Trp10	7.68	4.45	3.28, 3.11		7.16	10.02	H ζ : 7.40

Circular dichroism

Circular dichroism spectra were acquired on a Jasco Model J-1500 CD spectrometer at 25.0 °C. Wavelength scans were collected from 260 to 180 nm with a 1 nm bandwidth, 0.1 nm wavelength step, and an averaging time of 4 sec per step. The concentration of each peptide was 50 μM measured by UV-Vis absorbance at 280 nm.

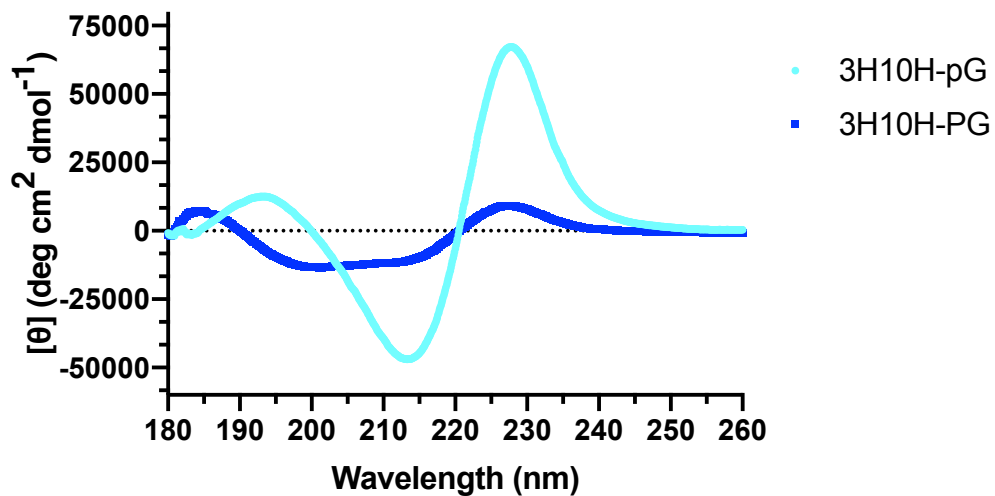


Figure S25. Circular dichroism of peptides **3H10H-pG** and **3H10H-PG**. The peptide **3H10H-pG** shows a spectral signature characteristic of beta-sheet secondary structure and the positive signal at 227 nm indicates the interaction between Trp aromatic chromophores,^{S2} providing further evidence of hairpin formation.

Peptide Characterization

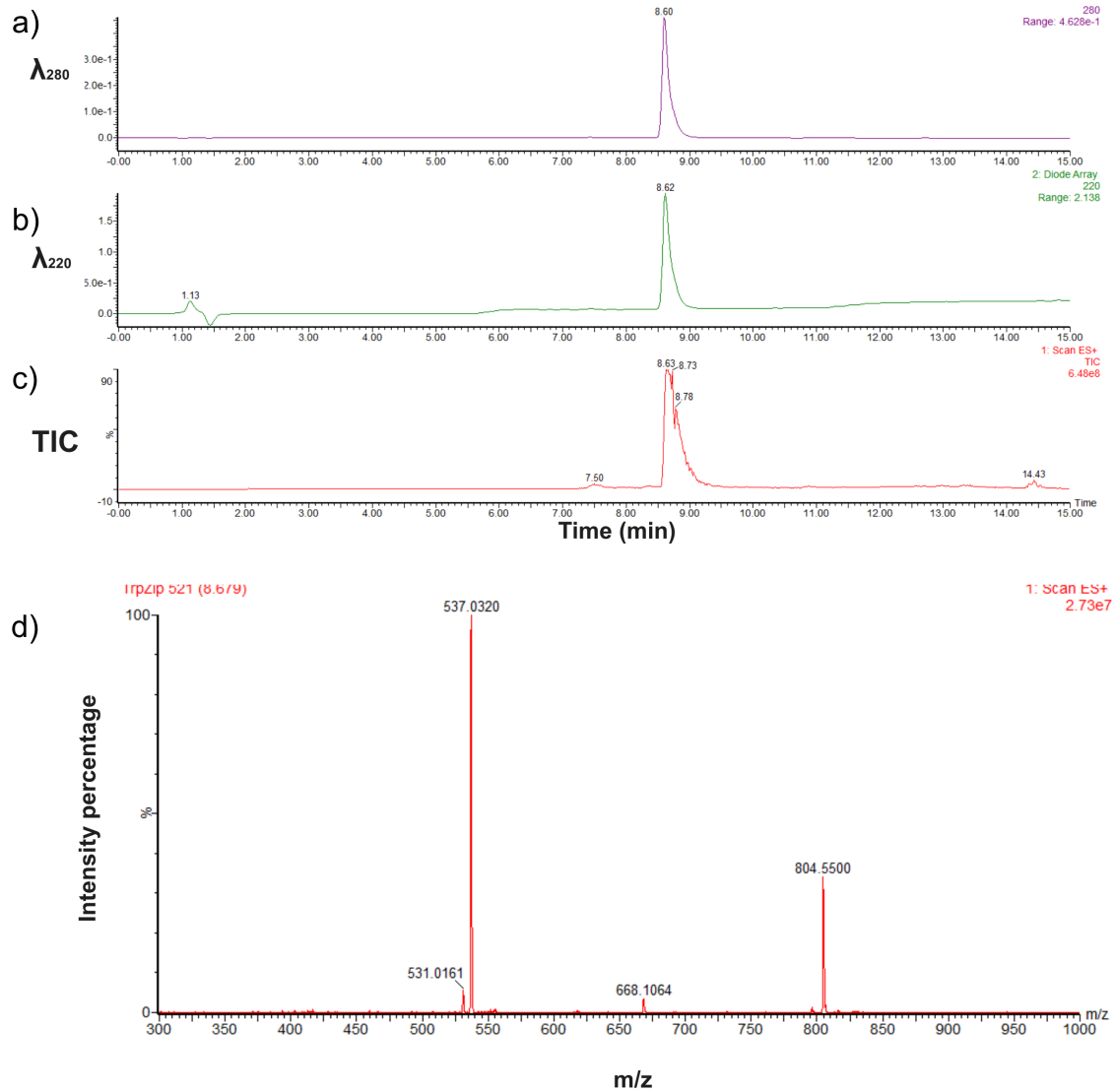


Figure S26. LCMS characterization of peptide **TrpZip**, sequence SWTWEGNKWTWK, showing a) absorbance at 280 nm, b) absorbance at 220 nm, c) the total ion chromatogram, and d) the mass spectrum of the main peak. $[M+3H]^{3+}$ calculated $m/z = 537.25$, found $m/z = 537.03$.

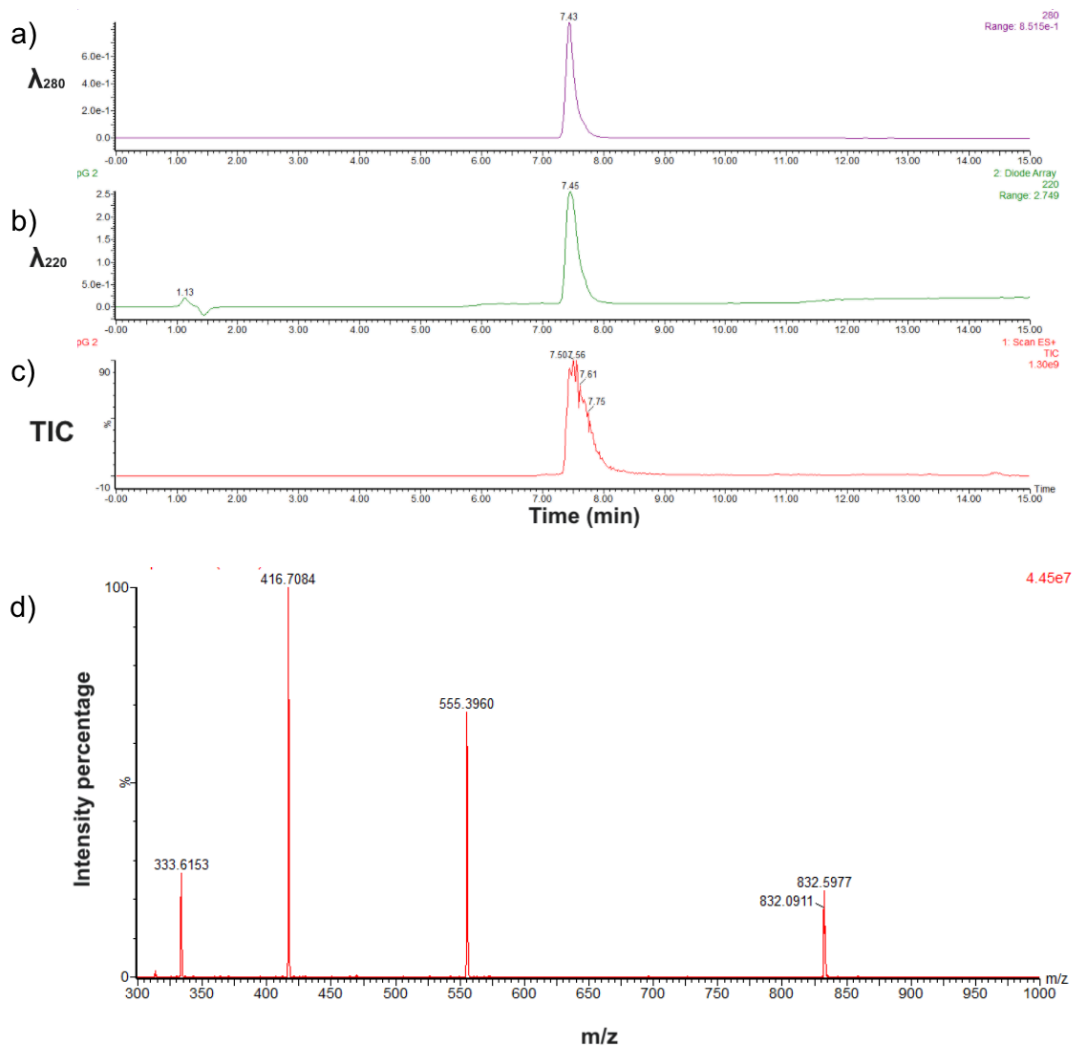


Figure S27. LCMS characterization of peptide **3H10H-pG**, sequence SWHWEpGKWHWK, showing a) absorbance at 280 nm, b) absorbance at 220 nm, c) the total ion chromatogram, and d) the mass spectrum of the main peak. $[M+3H]^{3+}$ calculated $m/z = 555.59$, found $m/z = 555.40$.

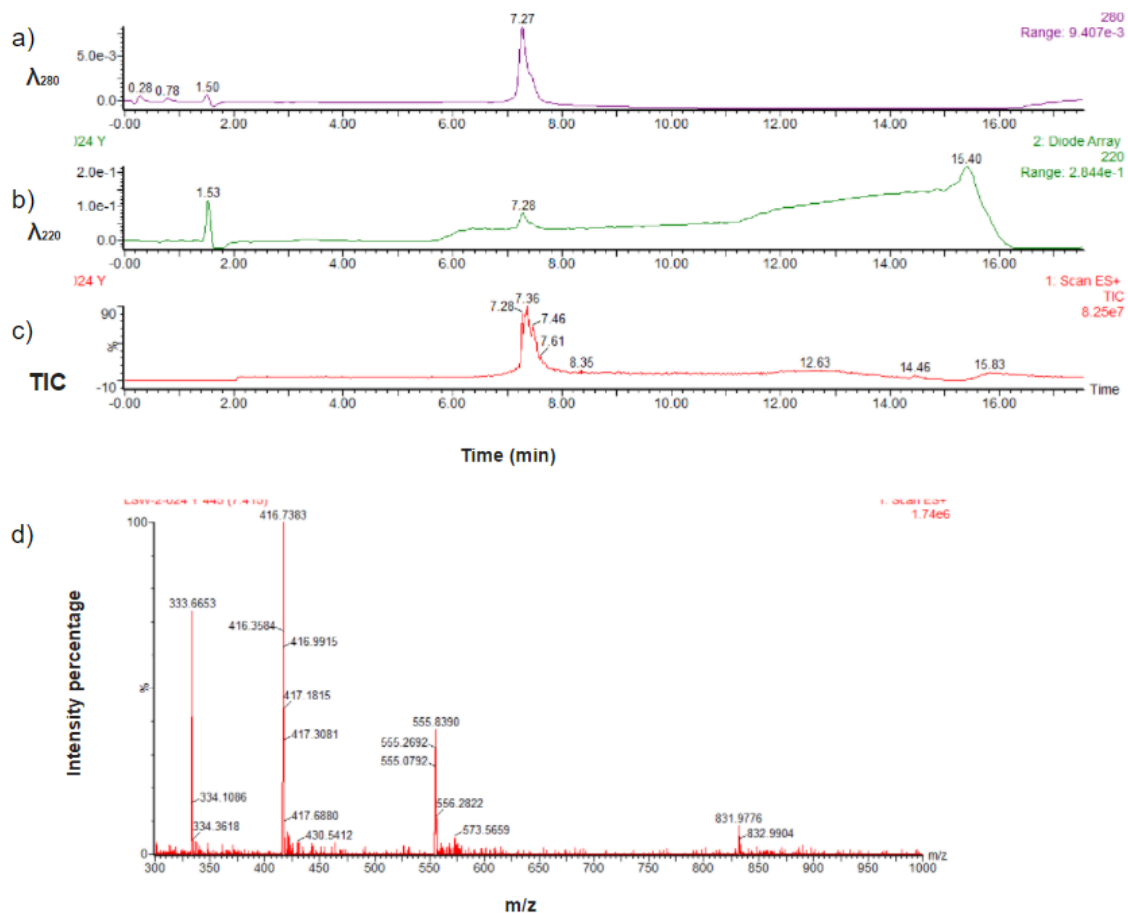


Figure S28. LCMS characterization of peptide **3H10H-PG**, sequence SWHWEPGKWHWK, showing a) absorbance at 280 nm, b) absorbance at 220 nm, c) the total ion chromatogram, and d) the mass spectrum of the main peak. $[M+3H]^{3+}$ calculated $m/z = 555.59$, found $m/z = 555.84$.

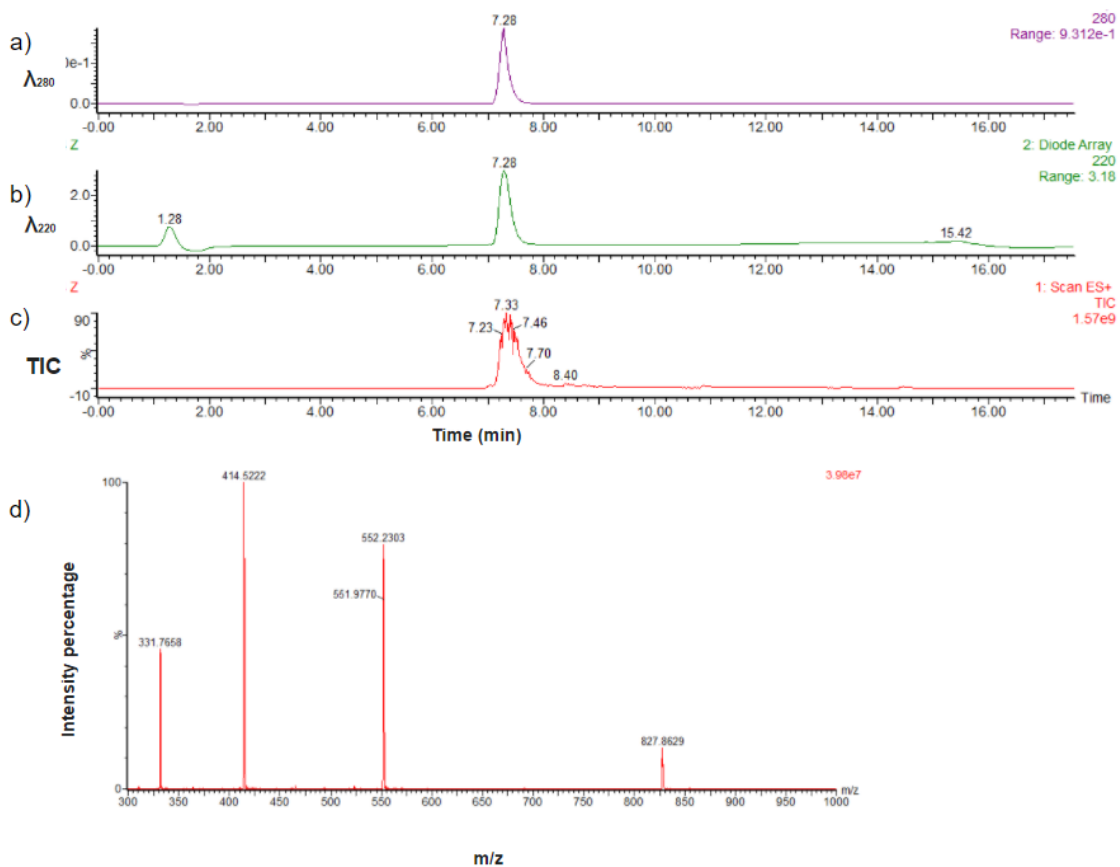


Figure S29. LCMS characterization of peptide **3H10K-pG**, sequence SWHWEpGKWKWK, showing a) absorbance at 280 nm, b) absorbance at 220 nm, c) the total ion chromatogram, and d) the mass spectrum of the main peak. $[M+4H]^{4+}$ calculated $m/z = 414.71$, found $m/z = 414.52$.

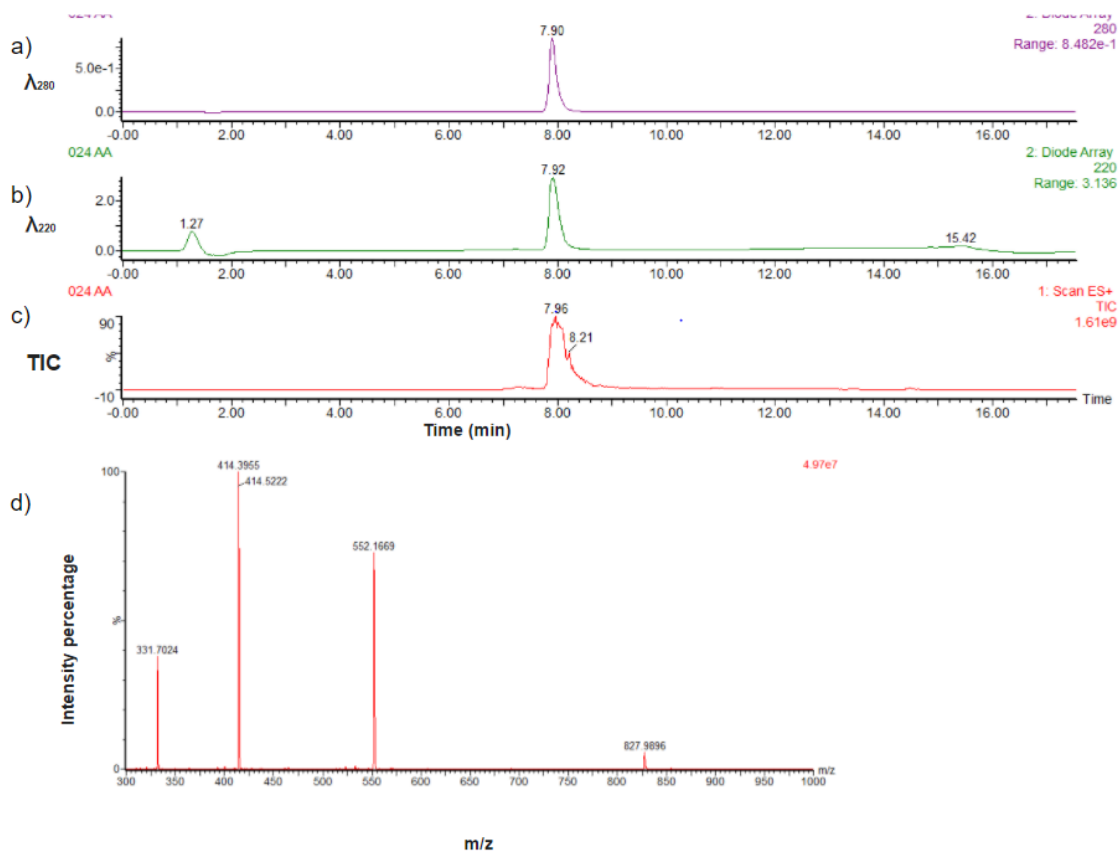


Figure S30. LCMS characterization of peptide **3H10K-PG**, sequence SWHWEPGKWKWK, showing a) absorbance at 280 nm, b) absorbance at 220 nm, c) the total ion chromatogram, and d) the mass spectrum of the main peak. $[M+3H]^{3+}$ calculated $m/z = 552.61$, found $m/z = 552.17$.

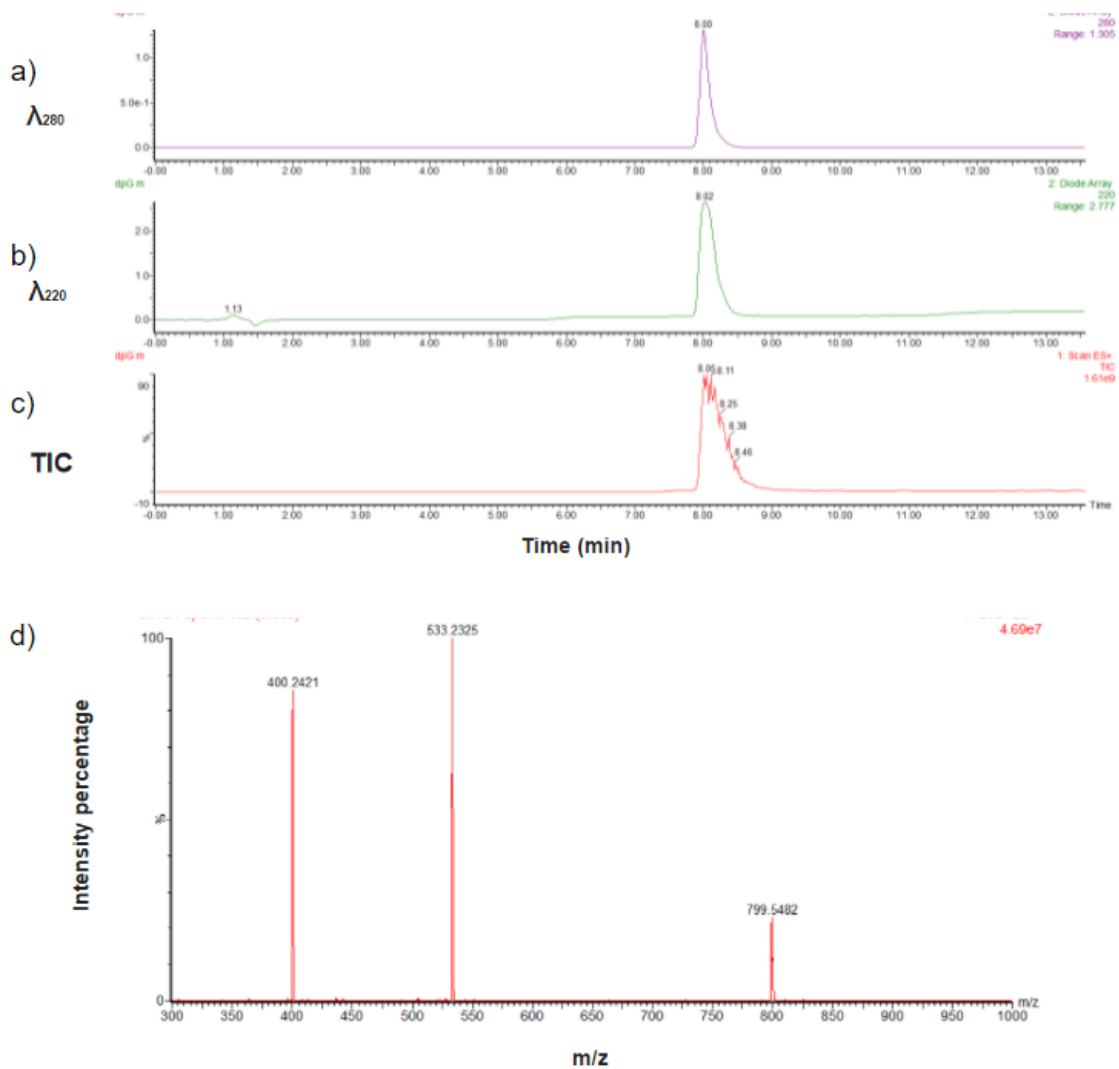


Figure S31. LCMS characterization of peptide **3H10A-pG**, sequence SWHWEpGKWAWK, showing a) absorbance at 280 nm, b) absorbance at 220 nm, c) the total ion chromatogram, and d) the mass spectrum of the main peak. $[M+3H]^{3+}$ calculated $m/z = 533.58$, found $m/z = 533.23$.

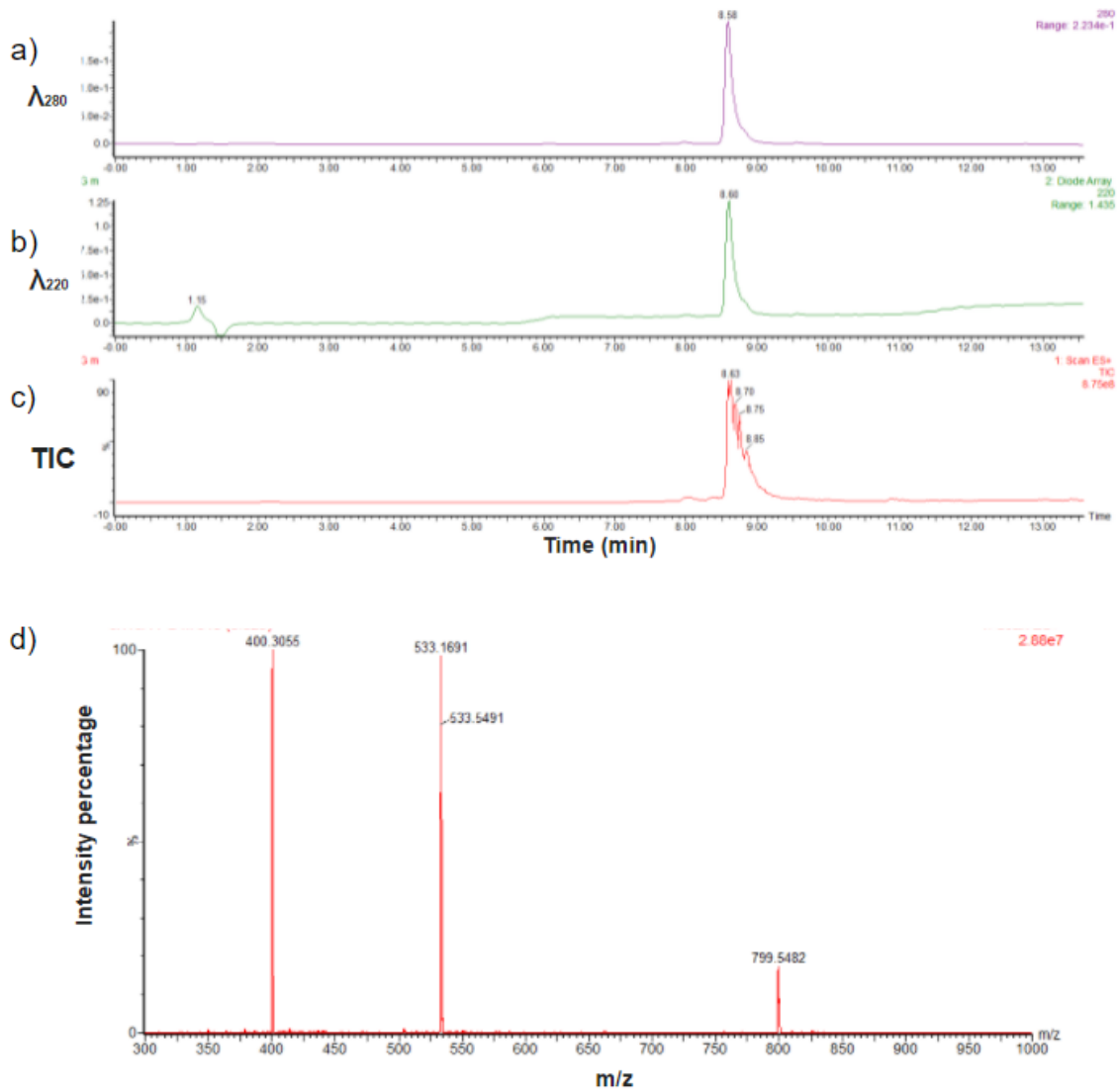


Figure S32. LCMS characterization of peptide **3H10A-PG**, sequence SWHWEPGKWAWK, showing a) absorbance at 280 nm, b) absorbance at 220 nm, c) the total ion chromatogram, and d) the mass spectrum of the main peak. $[M+4H]^{4+}$ calculated $m/z = 400.44$, found $m/z = 400.31$.

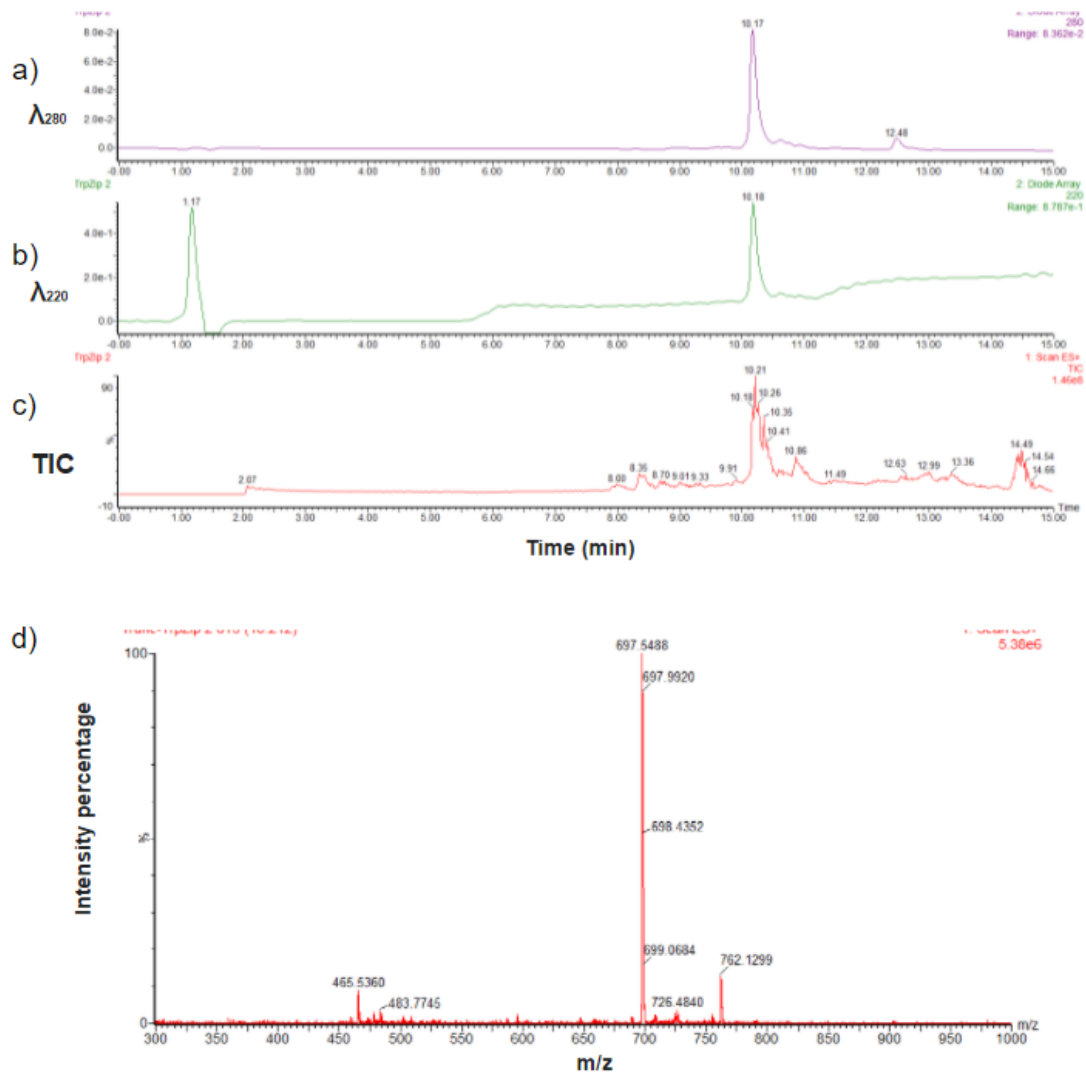


Figure S33. LCMS characterization of peptide **Trunc-TrpZip**, sequence WTWEGNKWTW, showing a) absorbance at 280 nm, b) absorbance at 220 nm, c) the total ion chromatogram, and d) the mass spectrum of the main peak. $[M+3H]^{3+}$ calculated $m/z = 465.54$, found $m/z = 465.54$.

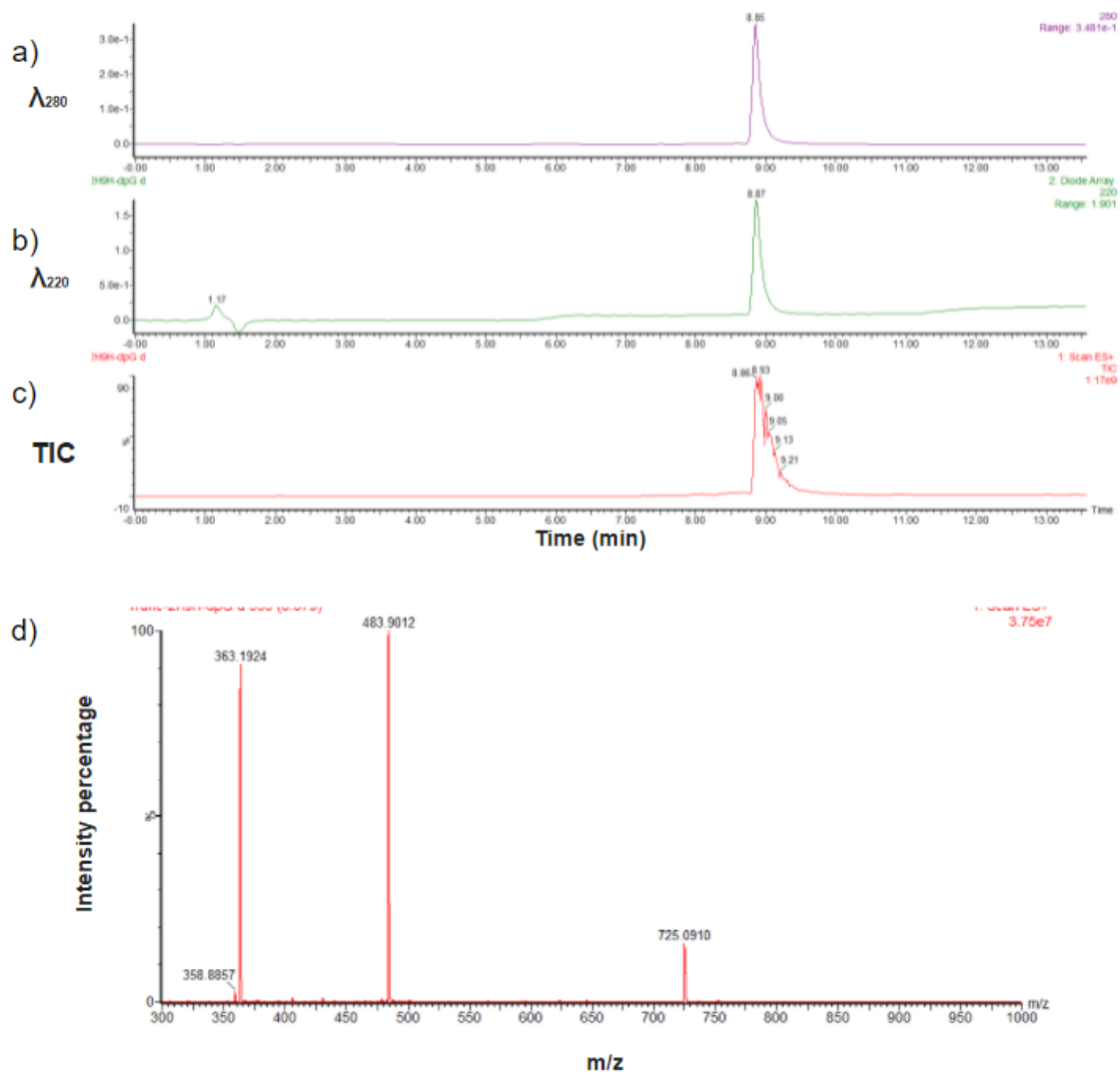


Figure S34. LCMS characterization of peptide **Trunc-2H9H-pG**, sequence WHWEpGKWHW, showing a) absorbance at 280 nm, b) absorbance at 220 nm, c) the total ion chromatogram, and d) the mass spectrum of the main peak. $[M+3H]^{3+}$ calculated $m/z = 483.89$, found $m/z = 483.90$.

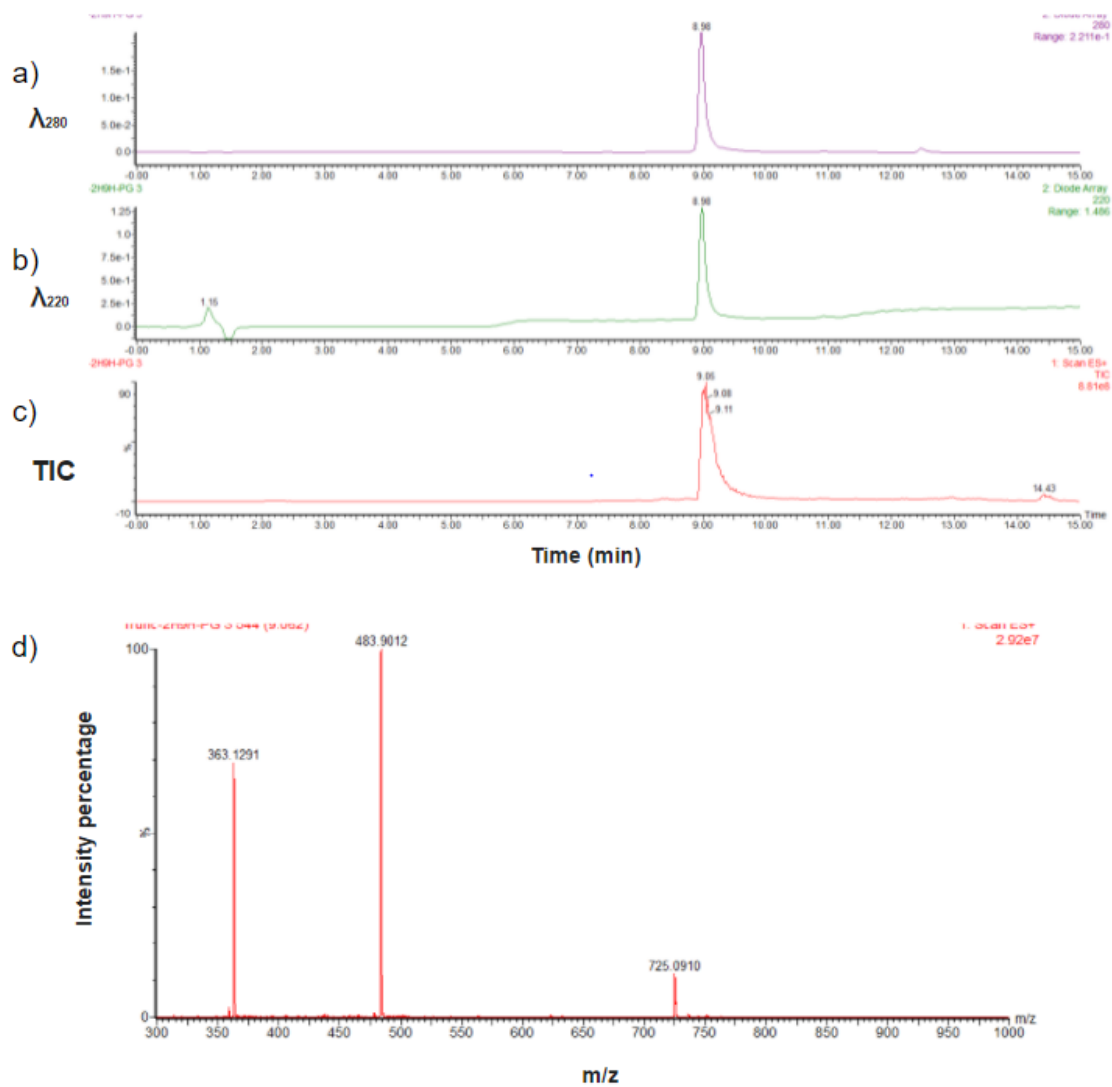


Figure S35. LCMS characterization of peptide **Trunc-2H9H-PG**, sequence WHWEPGKWHW, showing a) absorbance at 280 nm, b) absorbance at 220 nm, c) the total ion chromatogram, and d) the mass spectrum of the main peak. $[M+3H]^{3+}$ calculated $m/z = 483.89$, found $m/z = 483.90$.

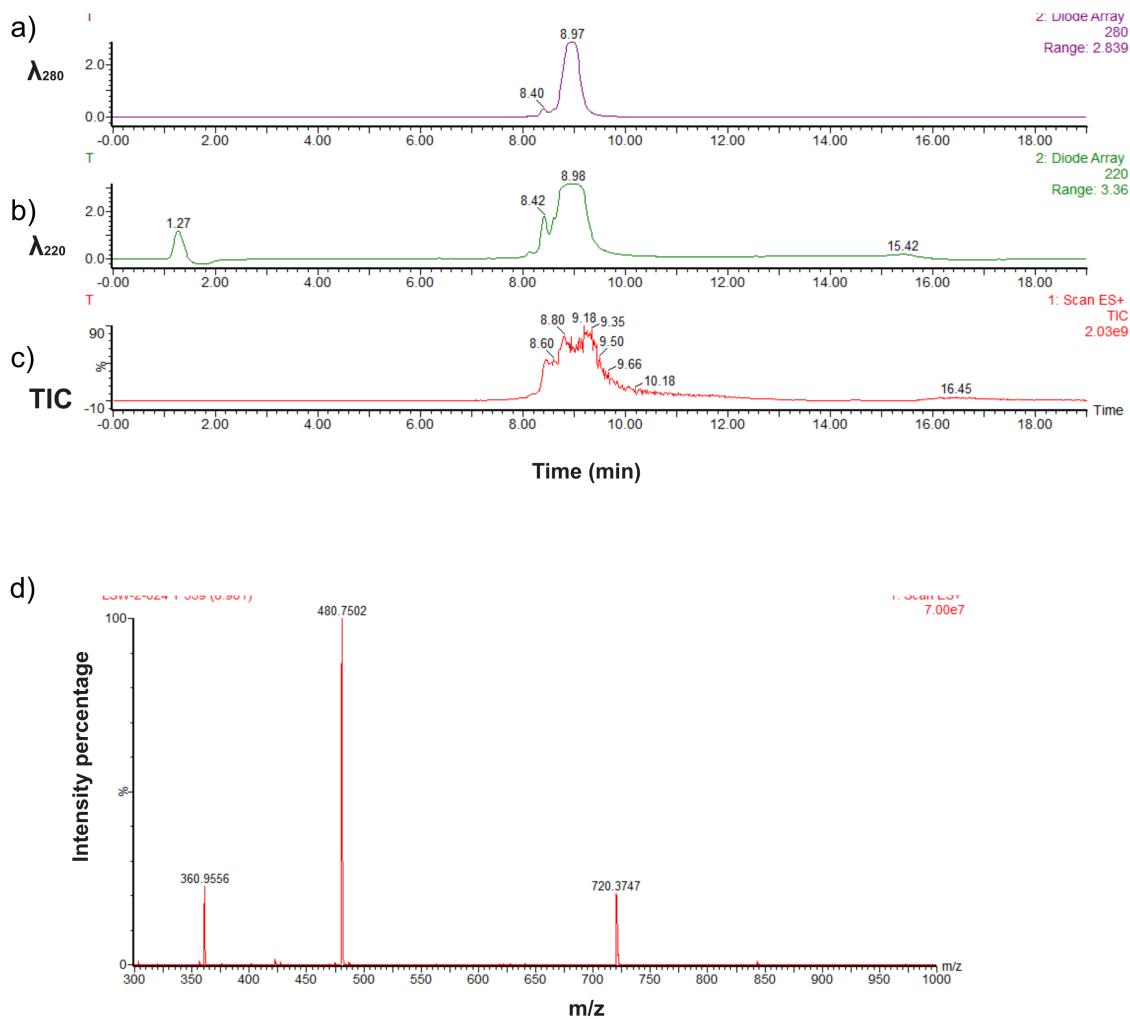


Figure S36. LCMS characterization of peptide **Trunc-2H9K-pG**, sequence WHWEpGKWKW, showing a) absorbance at 280 nm, b) absorbance at 220 nm, c) the total ion chromatogram, and d) the mass spectrum of the main peak. $[M+2H]^{2+}$ calculated $m/z = 720.85$, found $m/z = 720.37$.

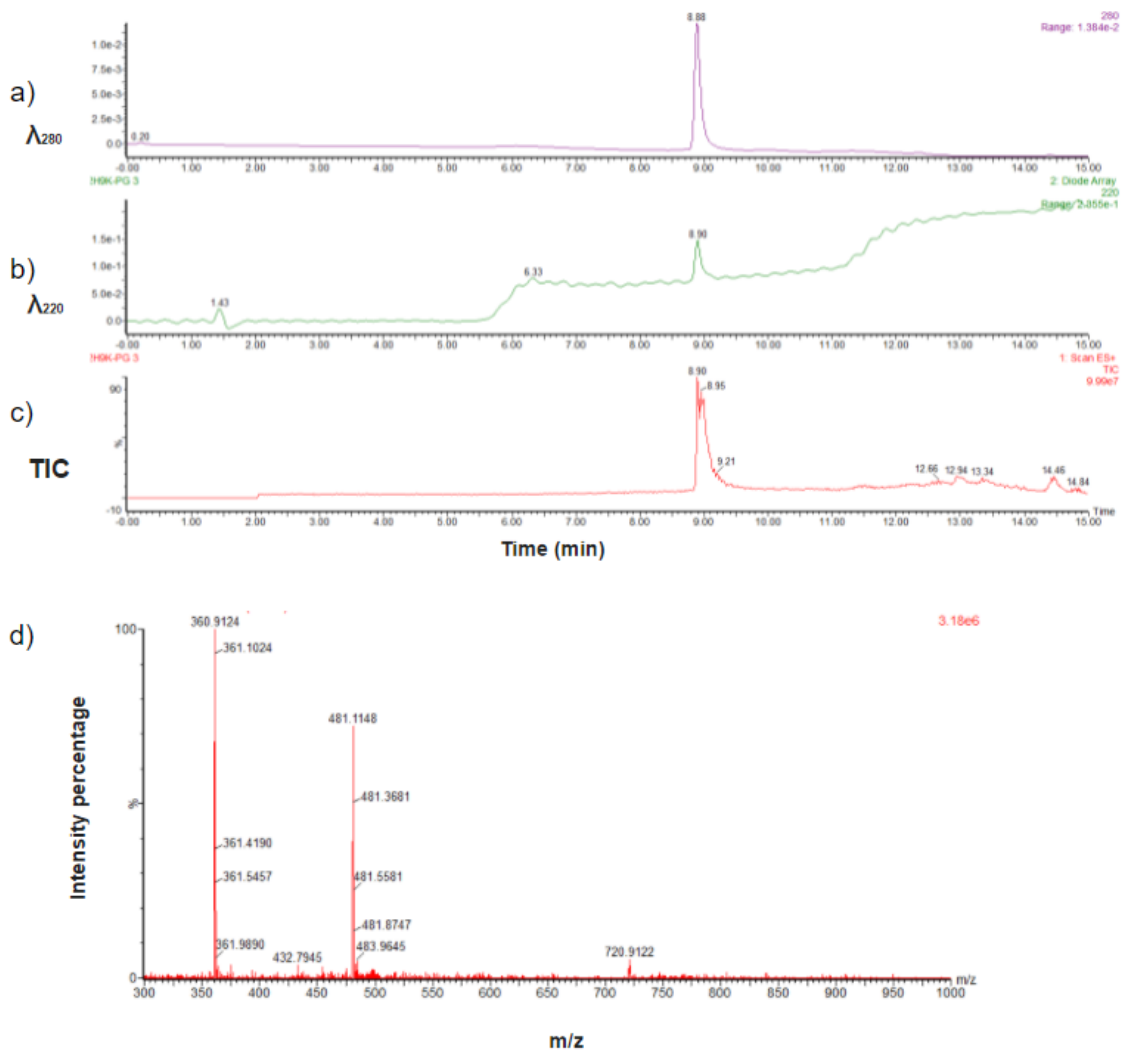


Figure S37. LCMS characterization of peptide **Trunc-2H9K-PG**, sequence WHWEPGKWKW, showing a) absorbance at 280 nm, b) absorbance at 220 nm, c) the total ion chromatogram, and d) the mass spectrum of the main peak. $[M+2H]^{2+}$ calculated $m/z = 720.85$, found $m/z = 720.91$.

Computational Models

Computational models were calculated for peptides **3H10H-pG** and **Trunc-2H9H-pG** using Robetta (<https://robetta.bakerlab.org/>), using the modeling method, RoseTTAFold.^{S3} The input sequences had multiple Gly residues (not shown in images) added to the N and C termini in order to satisfy the length limit in Robetta. Since Robetta does not support D-amino acids, the input β -turn was a Gly-Asn type II' β -turn, similar to the D-Pro-Gly turn used in our sequences.

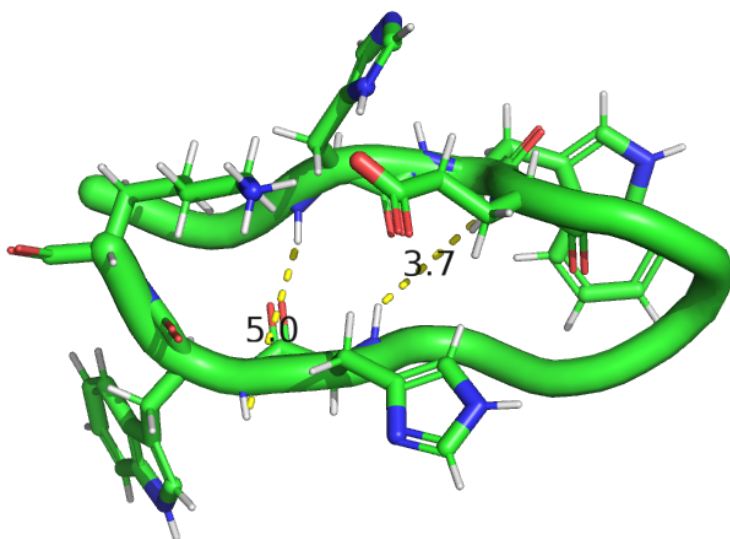


Figure S38. Robetta computational model of peptide **3H10H-pG** with backbone distances between protons observed to have NOE signals labeled.

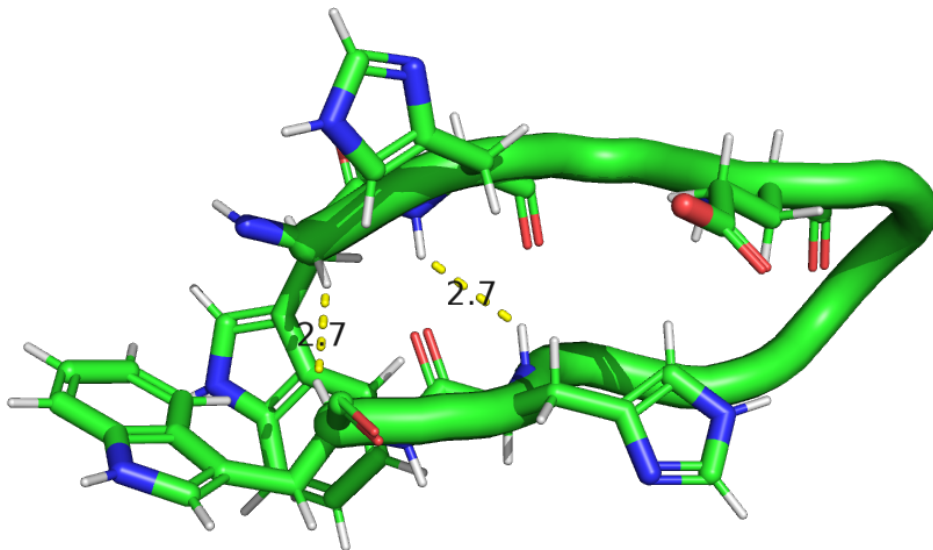


Figure S39. Robetta computational model of peptide **Trunc-2H9H-pG** with backbone distances between protons observed to have NOE signals labeled.

Supplemental references

S1. Lee, W.; Tonelli, M.; Markley, J. L. NMRFAM-SPARKY: enhanced software for biomolecular NMR spectroscopy. *Bioinformatics*. **2015**, *31*, 1325.

S2. I. B. Grishina and R. W. Woody, Contributions of tryptophan side chains to the circular dichroism of globular proteins: exciton couplets and coupled oscillators, *Faraday Disc.*, **1994**, *99*, 245.

S3. Kim, D. E.; Chivian, D.; Baker, D. Protein Structure Prediction and Analysis Using the Robetta Server. *Nucleic Acids Research* **2004**, *32*, W526–W531.